Ocean Sci. Discuss., https://doi.org/10.5194/os-2017-95
Manuscript under review for journal Ocean Sci.
Discussion started: 18 December 2017

Ocean Science Discussions

Estimating downwelling solar irradiance at the surface of the tropical Atlantic Ocean: A comparison of PIRATA measurements against several re-analyses and satellite-derived data sets

Mélodie Trolliet[1], Jakub P. Walawender[2], Bernard Bourlès[3], Alexandre Boilley[4], Jörg Trentmann[2], Philippe Blanc[1], Mireille Lefèvre[1], Lucien Wald[1]

[1] MINES ParisTech, PSL Research University, O.I.E. - Center for Observation, Impacts, Energy, Sophia Antipolis, France
[2] Deutscher Wetterdienst, Offenbach, Germany
[3] IRD/LEGOS, Brest, France
[4] Transvalor, Mougins, France

Correspondence to: Mélodie Trolliet (melodie.trolliet@mines-paristech.fr)

Running title: M. Trolliet et al.: Comparing PIRATA measurements, re-analyses and satellite-derived data.

Abstract.

This paper assesses the merits and drawbacks of several data sets of the solar downwelling radiation received at the surface of the tropical Atlantic Ocean where the field of solar radiation is hardly known. The data sets are compared to qualified measurements of hourly irradiance made at five buoys of the PIRATA network for the period 2012-2013. The data sets comprise the re-analyses MERRA-2 and ERA-5 and three satellite-derived data sets: HelioClim 3v5, SARAH 2 and CAMS Radiation Service v2. The re-analyses often report cloud-free conditions while actual conditions are cloudy and reciprocally, actual cloudless conditions as cloudy. The medium and high level clouds exhibit more bias than the low level clouds. The re-analyses poorly correlate with the optical state of the atmosphere derived from the measurements. The actual irradiance field is spatially distorted by re-analyses, especially for MERRA-2. Performances are similar between the three satellite-derived data sets. They correlate well with the optical state of the atmosphere and reproduce well the dynamics of the solar irradiance. The three data sets exhibit overestimation with the lowest biases reached by CAMS Radiation Service v2. The bias of HelioClim 3v5 is fairly similar from one location to the other which means that the actual spatial gradients are well reproduced.

Ocean Sci. Discuss., https://doi.org/10.5194/os-2017-95
Manuscript under review for journal Ocean Sci.
Discussion started: 18 December 2017

Introduction

The solar radiation impinging at the ocean surface is known to be an essential variable in the ocean-climate system (Budyko, 1969; Manabe, 1969; Siegel et al., 1995; Lean and Rind, 1998). The density of power received from the sun on a horizontal surface at ground level and per unit surface is called the downwelling solar irradiance at surface and is here abbreviated in DSIS. Other terms may be found in literature, such as solar exposure, solar insolation, solar flux, surface solar irradiance, downwelling shortwave flux, or surface incoming shortwave radiation. The DSIS intensity is large over the tropical Atlantic Ocean and influences the sea surface temperature. The net downward surface energy is positive and accumulates within the ocean with a resulting northward meridional transport of heat in the Atlantic Ocean (Liu et al., 2017). The DSIS influences the vertical structure at more rapid time scales with local impact on physics and plankton (Siegel et al., 1995).

Currently, the field of DSIS is hardly known in this area. One of the means to assess the DSIS is measuring stations such as pyranometers aboard ship or on buoys (Cros et al., 2004). Such measurements are usually accurate though the stations are sparse. They cannot offer a synoptic view of the field of the DSIS. Images acquired by satellites observing the ocean surface are a second means to getting a synoptic view of the temporal variations of the DSIS field. For example, the series of geostationary Meteosat satellites offer synoptic views of the tropical and equatorial Atlantic Ocean every 15 min with a spatial resolution between 3 and 5 km. Several data sets of DSIS have been constructed from these images, such as the HelioClim-3, SARAH-2 (Surface Radiation Data Set – Heliosat, version 2) and CAMS (Copernicus Atmosphere Monitoring Service) Radiation Service v2 (abbreviated in CRS) data sets which are dealt with here.

Re-analyses are a third means, in which weather forecasts models are used in a re-analysis mode to reproduce what was actually observed. They assimilate state variables such as temperature, moisture and wind. On the contrary, DSIS is diagnostic, i.e. it is derived from a radiative transfer model and depends on the representation of the whole set of radiatively active variables of the atmospheric column above the point. Hence, re-analysis estimates should not be mistaken with DSIS measurements, because they include the uncertainty of the models. Of interest here are the ERA-5 developed at the ECMWF (European Center for Medium-range Weather Forecasts) and the MERRA-2 (Modern-Era Retrospective Analysis for Research and Applications, version 2) of the NASA (National Aeronautics and Space Administration).

Despite the fairly recent availability of gridded data sets, their use is spreading outside the climate community and there is a need for validation effort for a more informed usage of these data in ocean sciences as a whole. This paper aims at establishing the merits and drawbacks of each of the five data sets when compared to qualified hourly and daily measurements of the DSIS performed by the PIRATA (Prediction and Research Moored Array in the Tropical Atlantic) network of moorings in the tropical Atlantic Ocean, here considered as a reference. The data sets are briefly presented in Section 1. The performances are expressed as usual statistical indicators and are presented in Section 2. The merits and drawbacks of each data set are discussed in Section 3. The size of the grid cell is typically 5 km for satellite-derived data set and 50 km for re-analyses; it is large compared to a single point and this difference is discussed in Section 3. How to access the data is described in the section “data availability”.

Ocean Sci. Discuss., https://doi.org/10.5194/os-2017-95
Manuscript under review for journal Ocean Sci.
Discussion started: 18 December 2017

1 Data and methods

1.1 The PIRATA measurements

The PIRATA network comprises eighteen meteo-oceanic buoys (Atlas type, progressively replaced by T-FLEX systems from 2015; refer to https://www.pmel.noaa.gov/gtmba/pirata for more information) located in the Atlantic Ocean, between the latitudes 19° S and 21° N (Bourlès et al. 2008). Each PIRATA buoy is equipped with an Eppley pyranometer mounted at a height of 3.8 m and that measures the DSIS. Values are recorded as 2 min averages. The sensors are deployed for about one year on average before replacement. Sensors are cleaned manually every trimester.

The measurements are subject to the same sources of uncertainty that their counterpart on a firm ground, such as incorrect sensor levelling, shading caused by close structures, dust, dew, water-droplets, bird droppings, miscalibration of sensors, electronic failures, time shifts in data loggers, maintenance mishandling, etc. (see e.g. Muneer and Fairooz, 2002). Some buoys experience accumulation of African dust, potentially leading to significant underestimation of the DSIS (Foltz et al., 2013). These authors have proposed correction for such buoys including sea-spray, natural and anthropogenic aerosols but limited to daily means of the DSIS.

Pyranometers view a complete hemisphere and must be horizontal for accurate measurements. This is not the case within the PIRATA network where a pyranometer is affected by the motions of the buoy which change the portion of the sky seen by the pyranometer, inducing errors in the measurement. The errors are very complex to estimate and correct (Katsaros and DeVault, 1986; MacWhorter and Weller, 1991). They depend on the relative sun-buoy geometry which may be expressed as the tilt angle the angle between the plane of the pyranometer and the horizontal and the difference in azimuth of the sun and tilt direction. This relative geometry is affected by wave action or strong surface current and depends on time of the day, latitude and season. Since the downward radiation received from a portion of the sky depends on the sky conditions, the errors depend also on sky conditions. Errors are most apparent in conditions of high DSIS, in cloudless skies, when solar zenithal angles are less than 60°. By the means of an analytical model, Katsaros and DeVault (1986) calculated the error on clear-sky days for tilts up to 10°, which are likely to occur frequently on buoys. Ignoring the reflection of the sun rays off the ocean, their calculations predict a relative error on daily average up to 10% in the tropical region. Instantaneous errors due to motions from waves can be as large, up to 10% for the hourly average for solar zenithal angles greater than 30°. The wave action and a preferential tilt have the least effect in the tropics. However, diurnal variations in cloudiness, which are typical at low latitudes, will make the compensating gains and losses uneven over the day, and will therefore result in a larger net diurnal error than seen (Katsaros and DeVault, 1986). MacWhorter and Weller (1991) experimentally confirmed these calculations with simultaneous measurements of irradiance by gimbaled and ungimbaled pyranometers. Systematic tilts of 10° induced by strong surface current or strong wind current yield relative errors in excess of 40%. Errors caused by wave action are less severe and may amount to 10%. Reynolds (2007) proposed an algorithm for correcting such errors. Inputs to this algorithm are the pitch, roll, and heading of the sensor as well as the relative contributions of the beam and diffuse

components to the global DSIS. Long et al. (2010) suggested a combination of a specific pyranometer and algorithm to achieve an accuracy of 10 W m-2 in 90% of the cases.

Currently, no correction is made to PIRATA measurements for these errors due to buoy tilt or soiling. Measurements of 2 min DSIS for the period 2004-2016 were downloaded from the web site of the PMEL (Pacific Marine Environmental Laboratory) of the NOAA (National Oceanic and Atmospheric Administration) of the USA. Quality flags are provided together with the measurements. The NOAA procedure for quality check rejects non plausible values, i.e. values exceeding 1400 W m 2. If any DSIS value, mean, standard deviation, or maximum, reads 0, all values are set to missing for that day. In a second pass, flags are raised if sensor outputs are zero or full scale all along the day, or if the daily mean of the DSIS is outside the interval [50, 325] W m 2, or if the maximum exceeds 1350 W m 2. In a third pass, a visual inspection and comparison with time series plots from neighboring sites are performed.

An additional quality control was performed at MINES ParisTech on the top of this NOAA screening for the sake of safety since the PIRATA measurements serve as reference in this comparison. The quality control used here is that of Korany et al. (2016) and comprises several tests of the 2 min DSIS against extremely rare limits and physically possible limits. Values falling outside the limits were excluded from the time-series for comparison. Eventually, a visual analysis was performed to further remove suspicious values. A noticeable fraction of the data was removed. Only measurements that passed all tests successfully were kept. The hourly mean of DSIS was computed by averaging the 30 measurements within this hour only if all measurements were declared valid. Otherwise, the hourly mean of DSIS was declared invalid.

Following the recommendations by Foltz et al. (2013), the buoys located north of 4° N were discarded because of the contamination by African dust and possible large occurrence of significant tilt due to currents. A further constraint in this study was the availability of enough measurements at each buoy with no major gap in a year to have an accurate description of the intra-year variability. In addition, the overlap with data sets impose to start the time period starts in 2010 as ERA-5 was only available for the period 2010-2016 at the instant of writing.

Eventually five buoys were offering enough hourly means of DSIS for the period 2012-2013 (Fig. 1, Table 1). In addition, the buoy 19s34w, offered also enough data in 2011, i.e. approximately 4200 measurements, and the buoys 0n10w and 6s10w had also enough data in 2010 and 2011. This ensemble of data for other years was used for further control of results and analyses.

Ocean Sci. Discuss., https://doi.org/10.5194/os-2017-95
Manuscript under review for journal Ocean Sci.
Discussion started: 18 December 2017

Station	Latitude (positive North)	Longitude (positive East)	Number of hourly values in the time-series	Hourly mean of DSIS (W m^{-2})	Hourly mean clearness index	Daily mean of DSIS (W m^{-2})	Daily mean clearness index
0n0e	0.0	0.0	8356	449	0.48	215	0.52
0n10w	0.0	-10.0	8417	480	0.52	232	0.56
0n23w	0.0	-23.0	7431	530	0.57	256	0.62
6s10w	-6.0	-10.0	8461	485	0.53	235	0.57
19s34w	-19.0	-34.0	8541	496	0.57	243	0.61

Table 1: Geographical coordinates of the PIRATA buoys used in this study, number of hourly values in each time-series, hourly mean of DSIS and mean clearness index for the period 2012-2013.

Let E be the hourly mean of DSIS and E0 the corresponding irradiance received on a horizontal plane located at the top of the atmosphere. The hourly clearness index KT is defined as the ratio of E to E0. E0 was computed here by the means of the SG2 algorithm (Blanc and Wald, 2012). Though KT is not completely independent of the position of the sun, the dependency of KT with the solar zenithal angle is much less pronounced than that of E. Hence, KT characterizes the optical state of the atmosphere better than E. KT is typically close to 0.8 in cloud-free conditions, and close to 0.1 in overcast conditions with optically thick clouds.

The daily means of DSIS were computed by summing up the hourly means and by dividing by 24 h. The daily clearness index was also computed in the same way than the hourly KT. Table 1 reports the hourly and daily mean of DSIS as well as the means of the hourly and daily clearness indices. The means of the daily KT are greater than 0.5 denoting that the selected stations experience large occurrences of cloud-free conditions. Table 1 shows a tendency for an increase in KT from East to West.

1.2 The HelioClim 3v5 data set (HC3v5)

HelioClim 3v5, abbreviated in HC3v5, is constructed by processing images of the Meteosat second generation satellites by the Heliosat-2 method (Rigollier et al., 2004; Lefèvre et al., 2007) modified by Qu et al. (2014). It covers Europe, Africa, Middle East, parts of South America and Atlantic Ocean (full Meteosat disc). It is available from 2004 up to now with a 15 min time step. The spatial resolution depends on the pixel position and is approximately 3 km in the tropical Atlantic Ocean. Data can be accessed through a web service at the SoDa Service (Gschwind et al., 2006). This web service performs itself the integration over time; together with the HC3v5 irradiances, it delivers the DSIS in cloud-free conditions as well as the irradiance at the top of atmosphere. These three quantities were downloaded as hourly means.

1.3 The SARAH-2 data set

The SARAH-2 data record (Pfeifroth et al., 2017a) is generated and distributed by EUMETSAT CM-SAF (Satellite Application Facility on Climate Monitoring). The data set has been obtained on the basis of observations from Meteosat first

and second generation using a Heliosat-based retrieval approach (Müller et al., 2015; Pfeifroth et al., 2017b). SARAH-2 provides information on the global and direct surface solar irradiance as well as the sunshine duration from 1983 to 2015 for the full Meteosat disc. The data is provided on a regular grid with a grid spacing of 0.05° x 0.05° as instantaneous values of the DSIS every 30 min and aggregated to daily and monthly averages. Here, the instantaneous values every 30 min were converted to hourly means by using the irradiance at the top of atmosphere.

1.4 The CAMS Radiation Service v2 data set (CRS)

The CAMS radiation service v2 data set, abbreviated in CRS, is generated by processing images of the Meteosat second generation by the Heliosat 4 method (Qu et al., 2017). The geographical and temporal coverages as well as the spatial and temporal resolutions are the same than HC3v5. Similarly to HC3v5, the hourly means of DSIS in actual and cloud-free conditions as well as the irradiance at the top of atmosphere were downloaded from the SoDa Service.

1.5 The MERRA-2 re-analysis data set

The MERRA-2 data set has many of the same basic features as the MERRA system (Rienecker at al., 2011) that has already been assessed against PIRATA daily means of the DSIS by Boilley and Wald (2015), but includes a number of important updates (Gelaro et al., 2017). MERRA-2 offers 72 vertical levels from ground to 0.01 hPa. The grid cell is 0.5° (approx. 55 km) in latitude by 0.625° (approx. 71.5 km at Equator) in longitude. The temporal coverage is 1980 up to now with 1 h time step. The hourly means of DSIS in actual and cloud-free conditions as well as the irradiance at the top of atmosphere were downloaded from the MERRA web site. The time series for each location of PIRATA buoys were constructed by firstly downloading the MERRA-2 time series for the nearest four surrounding grid cells and then by applying a spatial bilinear interpolation technique with a weighting factor that is inversely proportional to the distance to the PIRATA site.

1.6 The ERA-5 re-analysis data set

The ERA-5 is the fifth generation of ECMWF atmospheric re-analyses of the global climate, combining models with observations (Hersbach and Dee, 2016). It has several improvements compared to ERA. It has 137 levels from the surface up to 0.01 hPa. The size of the grid cell is 31 km. It is very recent and is being released by steps. At the moment of writing, the temporal coverage is 2010 up to now with 1 h time step. The period should be extended back to 1979 at the beginning of 2018. The hourly means of DSIS in actual and cloud-free conditions as well as the irradiance at the top of atmosphere have been downloaded from the ECMWF MARS web site. The time series for the buoys locations were constructed similarly to MERRA-2.

Ocean Sci. Discuss., https://doi.org/10.5194/os-2017-95
Manuscript under review for journal Ocean Sci.
Discussion started: 18 December 2017

1.7 The CAMS cloud classification

In addition to these datasets, other variables have been downloaded to support the analyses of the errors for each data set. The CAMS Radiation Service provides a classification of the clouds in four types as a function of the altitude (Qu et al., 2017):

- low level cloud: water cloud at low altitude, with a base height of 1.5 km and a thickness of 1 km;
- medium level cloud: water cloud at medium altitude, with a base height of 4 km and a thickness of 2 km;
- high level cloud: deep cloud of large vertical extent from low altitude to medium altitude, with a base height of 2 km and a thickness of 6 km;
- thin ice cloud: ice cloud with a base height of 9 km and a thickness of 0.5 km.

A verbose mode is available in this service from which one may download these cloud types and other variables such as the cloud coverage, solar zenithal angle or the aerosol optical properties.

2 Results

The present work followed the protocol that has been designed and is used in the framework of the CAMS to perform quarterly validation of the CRS products against qualified ground measurements (see reports from Lefèvre and Wald at https://atmosphere.copernicus.eu/validation-supplementary-products). It comprises two parts.

The first part consists in the computation of differences between estimates and measurements. These differences are then summarized by classical statistical quantities. In this part, one more constraint applies onto the PIRATA measurements: any measurement should be greater than a minimum significant value. This threshold is selected such that there is a 99.7% chance that the irradiance is significantly different from 0 and that it can be used for the comparison. It is set to 30 W m^{-2}, i.e. 1.5 times the uncertainty (percentile 95) of measurements of good quality as reported by the WMO (World Meteorological Organization, 2012). Otherwise, the measurement, and therefore the corresponding estimate, is not kept for the computation of the differences. Following the ISO standard (1995), the differences are computed by subtracting PIRATA measurements from the estimates. The set of differences is summarized by a few quantities namely the bias (mean of the differences), the standard deviation and the root mean square error. Relative values are computed relative to the mean of the corresponding PIRATA measurements for a given site. Correlation coefficients are computed. 2-D histograms between PIRATA measurements and estimates, also called scatter density plots, are drawn as well as histograms of the differences.

Statistical properties of estimates and measurements are compared in the second part. Histograms of both the PIRATA measurements and the estimates are computed, and are superimposed into a single graph. Such graphs aim at assessing the capability of a given data set to accurately reproduce the frequency distribution of the PIRATA measurements for the period. Monthly means and standard deviations within each calendar month of both the PIRATA measurements and the estimates are computed and displayed into a single graph.

Ocean Sci. Discuss., https://doi.org/10.5194/os-2017-95
Manuscript under review for journal Ocean Sci.
Discussion started: 18 December 2017

In addition to the protocol for CRS validation, other graphs have been drawn to study the dependency of the statistical indicators with the irradiance or the clearness index, and other variables such as the month, year, solar zenithal angle, cloud types, cloud coverage, water vapor content, the aerosol optical properties or month.

This enhanced protocol was applied to both *E* and *KT*. As for the performances of a model regarding its ability to estimate the optical state of the atmosphere, *KT* is a stricter indicator than *E* because it is less sensitive to changes induced by the changing geometry, namely the daily course of the sun and seasonal effects. These effects are usually well reproduced by models and lead to a *de facto* correlation between PIRATA measurements and estimates of *E*, hiding potential weaknesses of a model.

The protocol was first applied to each data set for the five buoys on the period 2012-2013, for hourly values. In order to better control and support the conclusions, it was also applied to:

- each data set for the five buoys on the period 2012-2013, for daily values, with a threshold of 7.5 W m^{-2} instead of 30 W m^{-2},
- each data set for the buoys: 0n10w and 6s10w for 2010-2011, and 19s34w in 2011, for both hourly and daily values.

Tables 2-4 report the correlation coefficients, biases and standard deviations of errors for each station and each data set for hourly and daily means for the period 2012-2013.

Station		HC3v5	SARAH-2	CRS	MERRA-2	ERA-5
0n0e	hourly	0.964 (0.865)	0.970 (0.877)	0.965 (0.882)	0.821 (0.486)	0.875 (0.606)
	daily	0.932 (0.927)	0.940 (0.935)	0.930 (0.925)	0.379 (0.355)	0.647 (0.599)
0n10w	hourly	0.952 (0.785)	0.965 (0.827)	0.958 (0.823)	0.858 (0.519)	0.901 (0.634)
	daily	0.874 (0.883)	0.898 (0.904)	0.898 (0.906)	0.328 (0.360)	0.547 (0.563)
0n23w	hourly	0.972 (0.811)	0.977 (0.832)	0.974 (0.829)	0.906 (0.562)	0.929 (0.641)
	daily	0.874 (0.881)	0.922 (0.926)	0.904 (0.908)	0.350 (0.386)	0.513 (0.544)
6s10w	hourly	0.968 (0.839)	0.978 (0.879)	0.970 (0.875)	0.893 (0.546)	0.896 (0.571)
	daily	0.920 (0.919)	0.945 (0.943)	0.925 (0.929)	0.485 (0.465)	0.479 (0.368)
19s34w	hourly	0.930 (0.645)	0.925 (0.627)	0.932 (0.662)	0.910 (0.560)	0.927 (0.640)
	daily	0.915 (0.803)	0.910 (0.795)	0.919 (0.813)	0.809 (0.584)	0.873 (0.705)

Table 2: Correlation coefficient observed at each PIRATA station for each data set for irradiance and clearness index in brackets

Ocean Sci. Discuss., https://doi.org/10.5194/os-2017-95
Manuscript under review for journal Ocean Sci.
Discussion started: 18 December 2017

Station		HC3v5	SARAH-2	CRS	MERRA-2	ERA-5
0n0e	hourly	48 (10 %)	55 (12 %)	31 (6 %)	-42 (-9 %)	25 (5 %)
	daily	23 (10 %)	27 (12 %)	15 (6 %)	-20 (-9 %)	13 (5 %)
0n10w	hourly	49 (9 %)	55 (11 %)	36 (7 %)	-17 (-3 %)	25 (5 %)
	daily	23 (10 %)	26 (11 %)	17 (7 %)	-8 (-3 %)	12 (5 %)
0n23w	hourly	30 (5 %)	27 (5 %)	17 (3 %)	-10 (-1 %)	-6 (-1 %)
	daily	14 (5 %)	12 (4 %)	7 (2 %)	-5 (-2 %)	-3 (-1 %)
6s10w	hourly	40 (8 %)	41 (8 %)	28 (5 %)	12 (2 %)	15 (3 %)
	daily	19 (8 %)	20 (8 %)	13 (5 %)	6 (2 %)	7 (3 %)
19s34w	hourly	31 (6 %)	11 (2 %)	10 (2 %)	23 (4 %)	-10 (-1 %)
	daily	15 (6 %)	5 (2 %)	5 (1 %)	11 (4 %)	-5 (-2 %)

Table 3: Bias (W m^{-2}) observed at each PIRATA station for each data set (relative values in brackets)

Station		HC3v5	SARAH-2	CRS	MERRA-2	ERA-5
0n0e	hourly	80 (17 %)	72 (16 %)	77 (17 %)	166 (36 %)	141 (31 %)
	daily	19 (8 %)	18 (8 %)	19 (8 %)	55 (25 %)	40 (18 %)
0n10w	hourly	93 (19 %)	79 (16 %)	86 (17 %)	151 (31 %)	128 (26 %)
	daily	22 (9 %)	20 (8 %)	20 (8 %)	52 (22 %)	38 (16 %)
0n23w	hourly	73 (13 %)	65 (12 %)	68 (12 %)	129 (24 %)	112 (21 %)
	daily	17 (6 %)	14 (5 %)	15 (5 %)	41 (16 %)	31 (11 %)
6s10w	hourly	77 (15 %)	62 (12 %)	74 (15 %)	134 (27 %)	132 (27 %)
	daily	18 (7 %)	15 (6 %)	17 (7 %)	41 (17 %)	41 (17 %)
19s34w	hourly	118 (23 %)	118 (23 %)	112 (22 %)	128 (25 %)	115 (23 %)
	daily	27 (11 %)	28 (11 %)	26 (10 %)	40 (16 %)	33 (13 %)

Table 4: Standard deviation of errors (W m^{-2}) observed at each PIRATA station for each data set (relative values in brackets)

The numbers in these Tables are discussed in Section 3. The correlation coefficients, biases and standard deviations of the errors for the hourly *E* and *KT* for the period 2012-2013 given in these Tables are similar or close to those for 2010 and 2011 (not presented). As expected, on may note that for a given data set and a given PIRATA site, the numbers in these Tables are consistent between hourly and daily values: the relative biases are the same for the hourly and daily means, and the standard deviations of errors are greater for hourly values than for daily values. As expected, the correlation coefficients for daily *E* are less than for hourly *E* because of the strong influence of the solar zenithal angle on the correlation coefficient which creates a *de facto* correlation of hourly values between estimates and measurements. As a consequence, the discussion in Section 3 will focus on the hourly values for the period 2012-2013. The other cases may be invoked on an *ad hoc* basis to underline divergences if any.

Ocean Sci. Discuss., https://doi.org/10.5194/os-2017-95
Manuscript under review for journal Ocean Sci.
Discussion started: 18 December 2017

3 Discussion

3.1 The HelioClim-3 v5 data set

The HC3v5 estimates correlate very well with the measurements. The correlation coefficient ranges between 0.93 and 0.97 for *E* and between 0.79 and 0.87 for *KT*, except at 19s34w (0.65) (Table 2). The bias for *E* is large and positive (overestimation). It ranges between 30 and 49 W m^{-2} (Table 3). Though a weak decrease from East to West may be detected in Table 2, the bias is almost the same for the five sites; the difference between the maximum and the minimum is 19 W m^{-2}. This indicates a systematic error that is fairly constant in space, meaning that the actual irradiance field is not noticeably distorted by HC3v5 and that the actual spatial gradients are well reproduced. Combined with the large correlation coefficients, this means that the time-series of the actual field of *E* are well reproduced though amplitudes of variation in space and time may be hampered by the large standard deviation of the errors that ranges between 77 and 93 W m^{-2}, with a much greater value (118 W m^{-2}) at 19s34w (Table 4). This finding is consistent with those of Bengulescu et al. (2017) who reported very high correlation coefficients between HC3v5 and in situ measurements at various temporal scales, from days to years.

The 2D histograms reveal a well aligned distribution with small scattering for both *E* and *KT* with an overall overestimation. Figures 2a and 2b exhibit the 2D histograms for the site 6s10w. The smallest irradiances less than 100 W m^{-2} are underestimated and those greater than 800 W m^{-2} exhibit much less overestimation and are more correctly estimated. HC3v5 calls upon the McClear model to estimate the DSIS in cloud-free conditions. This model exploits the properties of the atmosphere delivered by CAMS. The present results are consistent with several publications that have underlined the good quality of the McClear estimates when compared to high-quality measurements performed at terrestrial stations (Eissa et al., 2015; Lefèvre et al., 2013; Lefèvre and Wald, 2016; Marchand et al., 2017). The clearness indices for HC3v5 show a tendency to overestimate the actual *KT* and to underestimate the greatest *KT*. HC3v5 predicts too many cases of cloud-free when cloudy; the opposite case is also true but less frequently.

The frequency distributions of measurements are well reproduced by HC3v5 for *E* (see Fig. 3a for the site 6s10w), though one may note an overestimation of the frequencies in the range [800, 1000] W m^{-2} for stations 0n0e and 0n10w. As for *KT*, there is a tendency to a slight underestimation of frequencies by HC3v5 in the interval [0.4, 0.6] and an overestimation around 0.7 (see Fig. 3b for the site 6s10w). The monthly means of the estimated *E* overestimate those of the measurements at all sites, except in June and July when they are similar (November for 19s23w) (see e.g. Fig. 4a for the site 6s10w). The situation is more confuse for the monthly standard deviations which are similar or close for three stations and overestimated at the two other stations, except April to September when they are close.

As for the daily DSIS, the correlation coefficients for daily *KT* are greater than for hourly *KT*, close to 0.9 (0.80 at 19s34w), and similar to those for the daily *E* (Table 2). Contrary to the smallest hourly irradiances which are underestimated, the smallest daily irradiances (<300 W m^{-2}) are overestimated; otherwise they are well estimated (not shown). In conclusion,

HC3v5 produces correct daily estimates for cloud-free conditions but is mistaking fairly cloudy conditions as cloud-free from time to time.

Thomas et al. (2016a, b) have performed comparisons between hourly and daily HC3v5 estimates and measurements of *E* performed at a total of 44 Brazilian stations, i.e. at similar latitudes. Performances are fairly similar for both hourly and daily values. One may note that the bias for terrestrial sites is small and closer to 0 than for the PIRATA stations and that the standard deviations are a bit smaller. This may indicate some limitations in the accuracy of the PIRATA measurements.

3.2 The SARAH 2 data set

The SARAH-2 estimates correlate very well with the measurements. The correlation coefficient ranges between 0.93 and 0.98 for *E* and between 0.83 and 0.88 for *KT*, except at 19s34w (0.63) (Table 2). The bias for *E* is large and positive (overestimation). It ranges between 11 and 55 W m^{-2} (Table 3) with a tendency to decrease from East to West. This decrease may be related to the increase in *KT* from East to West shown in Table 1. The bias varies from site to site with a difference between the maximum and the minimum of 44 W m^{-2}. This indicates a systematic error that is not constant in space, meaning that the actual irradiance field may be spatially distorted by SARAH-2 and that the actual spatial gradients are not well reproduced. The standard deviation ranges between 62 and 79 W m^{-2}, with a much greater value (118 W m^{-2}) at 19s34w (Table 4). There is no clear relationship between the standard deviation and the frequency of clouds or *KT* or the geographical location. It may be concluded that the time-series of *E* are well reproduced though amplitudes of variation in time may be hampered by the large standard deviation of the errors.

As a whole, the SARAH-2 estimates reproduce well the coincident measurements with small scattering for both *E* and *KT* with an overall overestimation (see e.g. Figs. 2c, 2d). The smallest irradiances are underestimated and the greatest irradiances, i.e. greater than 800 W m^{-2}, exhibit much less overestimation and are more correctly estimated. SARAH-2 shows a tendency to overestimate the actual *KT* and to underestimate the greatest *KT*; it predicts too many cases of cloud-free when cloudy; the opposite case is also true but much less frequently.

The frequency distributions of SARAH-2 match well that of the measurements of *E* and differences are very small (see e.g. Fig. 3c). As for *KT*, there is a tendency to an underestimation of frequencies for $KT<0.5$ and an overestimation around 0.7 (see e.g. Fig. 3d). The monthly means of the estimated *E* overestimate those of the measurements at all stations, except 19s23w, and for all months at 0n0e and 0n10w, and all months but the period May-July for 0n23w and 6s10w (see e.g. Fig. 4b). The monthly standard deviations are similar or close for all stations and all months, except an overestimation in January-February at 0n0e and 0n10w.

As for the daily DSIS, the correlation coefficients for daily *KT* are greater than for hourly *KT*, greater than 0.90 (0.80 at 19s34w), and similar to those for the daily *E*. Contrary to the smallest hourly irradiances which are underestimated, the smallest daily irradiances (<300 W m^{-2}) are overestimated; otherwise they are well estimated. In conclusion, HC3v5 produces correct daily estimates for cloud-free conditions but is mistaking fairly cloudy conditions as cloud-free from time to time. Compared to the PIRATA distributions, the frequency distributions of daily *E* and *KT* from SARAH-2 are shifted

Ocean Sci. Discuss., https://doi.org/10.5194/os-2017-95
Manuscript under review for journal Ocean Sci.
Discussion started: 18 December 2017

towards the greatest *E* and *KT*, except at 19s23w where the distributions are close. In conclusion, SARAH-2 produces correct daily estimates for cloud-free conditions but is mistaking fairly cloudy conditions as cloud-free from time to time.

3.3 The CAMS Radiation Service data set (CRS)

The CRS data set correlates very well with the measurements. The correlation coefficient ranges between 0.93 and 0.97 for *E* and between 0.82 and 0.88 for *KT*, except at 19s34w (0.66) (Table 2). The bias for *E* is large and positive (overestimation) and ranges between 10 and 31 W m^{-2} (Table 3). The overestimation and range of bias are similar to those reported by Thomas et al. (2016a) for 42 stations in Brazil. This decrease may be related to the increase in *KT* from East to West shown in Table 1 and is in in agreement with the CAMS validation results quarterly reported by Lefèvre and Wald using terrestrial stations (https://atmosphere.copernicus.eu/validation-supplementary-products). Though it has not been discussed by these authors, one may note in their reports a tendency of the bias to decrease with an increase of the mean *KT*. The tendency is more visible for terrestrial stations where cloud-free conditions are often experienced like the selected PIRATA buoys. The bias varies from station to station in the PIRATA network with a difference between the maximum and the minimum of 26 W m^{-2}. The systematic error is not constant in space, and as a consequence the actual irradiance field may be spatially distorted by CRS and the actual spatial gradients may not be well reproduced. The standard deviation ranges between 68 and 86 W m^{-2}, with a much greater value (112 W m^{-2}) at 19s34w (Table 4). There is no clear relationship between the standard deviation and the frequency of clouds or *KT* or the geographical location. It may be concluded that that the time-series of *E* are well reproduced though amplitudes of variation in time may be hampered by the large standard deviation of the errors.

Coincident measurements are well reproduced by CRS as a whole with small scattering for *E* with an overall overestimation (see e.g. Fig. 2e). The smallest irradiances are underestimated and the greatest irradiances, i.e. greater than 800 W m^{-2}, are often correctly estimated. The clearness indices are overestimated as a whole with a noticeable scattering and the greatest *KT* are underestimated (see e.g. Fig. 2f). CRS predicts too many cases of cloud-free when cloudy; the opposite case is also true but much less frequently. Like HC3v5, CRS makes use of McClear to estimate the DSIS in cloud-free conditions. Though McClear offers accurate estimates, errors are possible in case of any gross errors in aerosol properties provided by CAMS. Other sources of errors found in cloud-free conditions originate from errors in the assessment of cloud properties (presence, coverage, optical depth).

The frequency distributions match well that of the measurements of *E* and differences are very small (see e.g. Fig. 3e). As for *KT*, all stations exhibit an overestimation of the frequencies around 0.6-0.7. 0n10w and 6s10w show a tendency to underestimate the frequencies for $KT<0.6$ (see e.g. Fig. 3f). Except 19s23w, there is an overestimation of the monthly means of *E* for all months except the period May-July during which no bias is observed (see e.g. Fig. 4c). At 19s23w, there is no bias except an overestimation in May-August. The monthly standard deviations are similar or close for all months at 0n23w and 19s34w, and similar or close for the other three stations with an overestimation in October-February.

Ocean Sci. Discuss., https://doi.org/10.5194/os-2017-95
Manuscript under review for journal Ocean Sci.
Discussion started: 18 December 2017

As for the daily DSIS, the correlation coefficients for daily *KT* are greater than for hourly *KT*, greater than 0.91 (0.81 at 19s34w), and similar to those for the daily *E*. In conclusion, CRS produces correct daily estimates for cloud-free conditions but is mistaking fairly cloudy conditions as cloud-free from time to time.

3.4 The MERRA-2 re-analysis data set

The MERRA-2 estimates do not correlate with the PIRATA measurements: the correlation coefficient ranges between 0.82 and 0.91 for *E* and between 0.49 and 0.56 for *KT* (Table 2). The latter coefficients are moderate and mean that at most 31% of the variance contained in the measured clearness indices is explained by MERRA-2. One may note that the correlation coefficients, both in *E* and *KT*, exhibit a tendency to increase from East to West. In addition, a dependency was found between the errors and the differences between the true solar time and the mean solar time. MERRA-2 does not account for this difference which is a function of the day in the year as a first approximation (Wald, 2007). This weakens *de facto* the correlation between the two series of data and increases the standard deviation of the errors for both hourly and daily values of *E* and *KT*.

The bias for *E* ranges between -42 and 23 W m^{-2} (Table 3). It shows a tendency to increase (from negative to positive) from East to West. The dependency of the bias with the solar zenithal angle and other variables is weak, except for the cloud type whose influence is prominent.

Fig. 5 shows the dependency of the bias and of the correlation coefficient as a function of the cloud type. One observes in Fig. 5a yellow and greenish tones, meaning negative and null bias, for the 'low-level' type (water cloud at low altitude) and 'thin' type (thin ice cloud), and blueish tones, meaning large positive bias for the 'medium-level' (water cloud at medium altitude) and 'high-level' (deep cloud of large vertical extent from low altitude to medium altitude). Fig. 5b shows that the correlation coefficients are similar or very close for all stations (each row is fairly uniformly colored) and that there is a dependency with the cloud type. Though a more detailed study with more cases is necessary, it can be speculated that the medium and high level clouds exhibit more bias and less correlation than the low level clouds. This is consistent with the preliminary findings of Doddy et al. (2017) who looked at the differences between measurements of daily *E* performed at terrestrial stations in Ireland and MERRA-2 outputs and suggested a systematic link between prevailing cloud structures and errors. A similar dependency of the errors with the mean *KT* has been reported by Zhao et al. (2013) for MERRA in North America. The bias varies from station to station with a difference between the maximum and the minimum of 65 W m^{-2}. This indicates that the systematic error is not constant in space, meaning that the actual irradiance field in the tropical Atlantic Ocean may be spatially distorted by MERRA-2 and that the actual spatial gradients may not be well reproduced. The standard deviation ranges between 128 and 166 W m^{-2} (Table 4) and exhibits a tendency to decrease with the regional increase in the mean *KT* (Table 1). Combined with the tendency of the correlation coefficient to increase with the mean *KT*, i.e. with increasing occurrence of cloud-free conditions, it may be speculated that MERRA-2 is as a whole more accurate in cloud-free conditions that in other conditions. This is in agreement with the findings of Kennedy et al. (2011), Yi et al. (2011), Zib et al. (2012), Zhao et al. (2013) or Boilley and Wald (2015) for MERRA.

The 2D histograms show that the dots for *E* are fairly well aligned along the 1:1 line with a very large scattering (see e.g. Fig. 2g). One may note a large underestimation of the greatest *E*. Close examination of randomly selected individual daily profiles of the MERRA-2 DSIS for cloud-free conditions against those from McClear has revealed that hourly means of irradiance are very similar in such conditions. Hence, the MERRA-2 cloud-free DSIS are likely accurate and the underestimation of the greatest *E* is mostly due to errors in prediction of cloud properties by MERRA-2. This is in agreement with the analysis of the 2D histograms for *KT* (see e.g. Fig. 2h). The shape of the 2D histogram is not elongated at all with a tendency to overestimate *KT* and a well-marked underestimation of the greatest *KT*.

The frequency distributions of measurements are fairly well reproduced for *E*, with an underestimation of the frequencies for the greatest *E* (see e.g. Fig. 3g). As for *KT*, one may note that the actual dynamics of *KT* is not fully covered by MERRA-2; the greatest values are not represented (see e.g. Fig. 3h). The situation is not the same for all sites. There is an overestimation of frequencies in the range [0.45, 0.65] ([0.6, 0.75] for 19s34w).

There is no systematic deviation in monthly means for all stations; the situation varies from station to station (Fig. 4d). The standard deviation is often underestimated. This is in agreement with the underestimation of the frequencies of the greatest *KT*.

As for the daily DSIS, the correlation coefficients for daily *E* are low: from 0.33 to 0.49 (0.81 for 19s34w), and are much less than those for hourly *E*, more than what is observed for the other data sets (Table 2). As for the daily *KT*, the coefficients are very low: from 0.36 to 0.47 (0.58 for 19s34w). At most 22% (34% for 10s34w) of the variance contained in the measured daily *KT* is explained by MERRA-2. There is no regional trend of the correlation coefficients. The 2D histograms have shapes which are not elongated and exhibit very large scattering, in full agreement with the low correlation coefficients. *E*, respectively *KT*, is sometimes overestimated but more frequently underestimated, especially the greatest *E*, respectively *KT*. Like for hourly values, the results indicates that the actual spatial gradients of daily DSIS are not well reproduced and that the actual field of daily DSIS may be spatially distorted by MERRA-2. This fact is recognized by Koster (2015) whose Figure 4.6 shows the difference between the yearly means of the DSIS between MERRA-2 and CERES (Clouds and the Earth's Radiant Energy System) EBAF (Energy Balanced and Filled) satellite-based observational dataset. In this picture, one may see a noticeable difference between both data sets. It ranges from -20 W m^{-2} in the Gulf of Guinea to 20 W m^{-2} along the Brazilian coast and exhibits structures that are compatible with our findings.

The fact that there is no systematic trend in monthly means and standard deviation may indicate that the spatial distortion occurs at various temporal scales. This is supported by the findings of Bengulescu et al. (2017). These authors performed a comparison between several data sets, among which HC3v5 and MERRA-2, and in situ measurements made at Vienna (Austria) and Kishinev (Moldova). They reported a very high correlation coefficient between MERRA-2 and in situ measurements (0.97 and 0.97 respectively) and showed that this high correlation was mostly due to the very high correlation coefficient between MERRA-2 and in situ measurements at the yearly period (0.99 in both stations), i.e. MERRA-2 reproduces well the seasonal variability. For any period less than 1 year, the correlation coefficient is only moderate and is

Ocean Sci. Discuss., https://doi.org/10.5194/os-2017-95
Manuscript under review for journal Ocean Sci.
Discussion started: 18 December 2017

less than 0.8, i.e. less than 64% of the variance of the estimates, indicating that MERRA-2 does not reproduce the variability observed in measurements for these periods.

3.5 The ERA-5 re-analysis data set

The ERA-5 estimates do not correlate with the measurements as well as the satellite-derived data sets: the correlation coefficient ranges between 0.88 and 0.93 for *E* and between 0.57 and 0.64 for *KT* (Table 2). The latter coefficients are moderate and mean that at most 41% of the variance contained in the measured clearness indices is explained by ERA-5. The standard deviation of errors ranges between 112 and 141 W m^{-2} (Table 4). The standard deviation exhibits a clear decreasing trend from East to West.

The bias for *E* ranges between -10 and 25 W m^{-2} (Table 3) and exhibits a regional tendency to decrease in absolute values and to tend to underestimation with increasing mean *KT* (Table 1). However, such a complex behavior can only be speculated given the small number of sites. The bias varies from site to site with a difference between the maximum and the minimum of 35 W m^{-2}. This indicates that the systematic error that is not constant in space. The actual irradiance field in the tropical Atlantic Ocean may be spatially distorted by ERA-5 and the actual spatial gradients may not be well reproduced. This is further supported by the strong dependency of the bias with the cloud type. Fig. 5 shows the dependency of the bias (Fig. 5c) and of the correlation coefficient (Fig. 5d) as a function of the cloud type. The medium and high level clouds exhibit more bias and less correlation than the low level clouds.

The 2D histograms show that the dots for *E* are aligned along the 1:1 line with a large scattering (see e.g. Fig. 2i). One may note a large underestimation of the greatest *E*, i.e. greater than 800 W m^{-2}. We may speculate from these 2D histograms that the DSIS for cloud-free conditions is underestimated. This is supported by the analysis of the 2D histograms for *KT* whose shapes are not elongated at all with a tendency to overestimation for $KT<0.6$ and a well-marked underestimation for $KT>0.6$ (see e.g. Fig. 2j). This has yet to be confirmed as ERA-5 is not providing estimates of the DSIS for cloud-free conditions contrary to MERRA-2.

The frequency distributions of measurements are fairly well reproduced for *E*, with an underestimation of the frequencies for the greatest *E* (see e.g. Fig. 3i). As for *KT*, one may note that the actual dynamics of *KT* is not fully covered by ERA-5; the smallest and greatest values are not represented (see e.g. Fig. 3j). There is an underestimation of frequencies for all values of *KT*, except an overestimation in the range [0.45, 0.65] for all stations.

There is no systematic deviation in monthly means for all stations; the situation varies from station to station (see e.g. Fig. 4e). The standard deviation is often underestimated. This is in agreement with the underestimation of the frequencies of the greatest *KT* (see e.g. Fig. 3j).

As for the daily DSIS, the correlation coefficients for daily *E* are low: from 0.48 to 0.65 (0.87 for 19s34w), and expectedly are less than those for hourly *E*. The correlation coefficients for the daily *KT* are low: from 0.37 to 0.60 (0.71 for 19s34w). At most 36% (50% for 10s34w) of the variance contained in the measured daily *KT* is explained. Except 19s34w, the 2D

histograms have shapes which are not elongated and look more like discs, and exhibit large scattering, in full agreement with the low correlation coefficients.

3.6 About the differences in spatial support of the buoy and the grid cell of the data sets

One may object that the size of the grid cell is inappropriate for the comparison with a single buoy because surface measurements are for a single point in space, whereas the estimated irradiances are for the area of a pixel (typically 5 km) or a grid cell (typically 50 km). Cloud properties may vary within the grid cell and large random errors are unavoidable at hourly time step. Using monthly averages is a means to reduce the errors caused by the problem (see e.g. Zhao et al., 2013). One may believe that this mismatch in spatial support of information may explain the performances of the re-analyses presented here. However, it can be argued that there is no orographic effect in the Atlantic Ocean and there is no strong systematic gradient in irradiance over short distance corresponding to the hourly time step. Hence, the irradiance field is fairly homogeneous at sub-meso-scale and this should mitigate the effects of the differences in spatial support of the buoy and the grid cell. In addition, one may note that the drawbacks reported above are also observed at daily scale. Finally, the work of Boilley and Wald (2015) can be mentioned. These authors compared the satellite-derived HelioClim-1 data set to PIRATA measurements. HelioClim-1 is fairly similar to the re-analyses with regard to the spatial support of information because it is made of estimates of the DSIS made on 5 km pixels spaced by 25 km in both latitude and longitude (Lefèvre et al., 2007, 2014), and a spatial bi-linear interpolation was performed to create the time-series at PIRATA locations. Though the period is not the same than presently as HelioClim-1 covers the period 1985-2005, one may compare the correlation coefficients reported by these authors that range between 0.82 and 0.88 for daily E and from 0.79 to 0.88 for daily KT for HelioClim-1, and are much greater than those obtained for the re-analyses both in the work of Boilley and Wald and here (Table 2). These findings of Boilley and Wald support the argument that differences in spatial support of information cannot be the only reason for the bad performances of the re-analyses.

Conclusions

It was found that the re-analyses MERRA-2 and ERA-5 often report cloud-free conditions while actual conditions are cloudy, yielding an underestimation of surface irradiance, and reciprocally, actual cloudless conditions as cloudy, yielding an overestimation. These alternating underestimations and overestimations compensate each other with a small bias as a result masking some deficiencies in properly modelling cloud properties. These conclusions are similar to those already reported regarding meteorological re-analyses as a whole (Wild, 2008). The estimates from MERRA-2 or ERA-5 poorly correlate with the clearness indices at station; a large part of the variability in the optical state of the atmosphere is not captured by the MERRA-2 or ERA-5 re-analyses. It is recommended not to use them in studies of the variability in time of the surface irradiance in the tropical Atlantic Ocean when it is necessary to reproduce actual measurements.

The bias varies noticeably with the calendar month, which means that MERRA-2 or ERA-5 cannot be used confidently at monthly scale. The re-analyses exhibit small bias when compared to PIRATA measurements over one or more years. Hence, one may use them to follow changes in yearly values of irradiance at one location. However, caution must be taken as Zhao et al. (2013) reported correlation coefficients between yearly means of MERRA and observations ranging from 0.50 (moderate anti-correlation) to 0.95 (high correlation) at several sites in North America.

Another striking feature is the variability of the bias and other performance indicators within this ocean area which is fairly homogeneous for the irradiance and clearness index. Accordingly, an additional recommendation on re-analyses is not to use them to study the irradiance spatial field at whatever time scale: the performances strongly vary from one location to another, especially for MERRA-2, which means that the field of surface irradiance is spatially distorted, even at yearly scale.

The present results bring more evidence on the qualities and limitations of MERRA-2 and ERA-5. These re-analyses may be used in studies of the tropical Atlantic Ocean with proper understanding of the limitations and uncertainties. Zhao et al. (2013) proposed an empirical relationship for correcting the bias observed between MERRA estimates and measurements of monthly averages of irradiance performed at several sites in North America taking into account the dependency between the bias and KT and surface elevation. The bias and the root mean square error were reduced but at the expenses of an increase in standard deviation of errors. Jones et al. (2017) have tested several methods for adjusting ERA-Interim estimates of E onto HC3v5. They found that when compared to measurements of daily irradiance performed at 55 terrestrial stations in Europe, the bias was reduced for 10 stations and similar for the others and that the other indicators (standard deviation of errors, root mean square error, correlation coefficient, median of errors…) were unchanged. Though the works were performed for MERRA or ERA-Interim, it is speculated that similar conclusions would be reached when applied to MERRA-2 or ERA-5, given the similarities between these re-analyses.

Except for the bias, the three satellite-derived data sets exhibit better performance indicators than the two re-analyses. All three overestimate the irradiance. Assuming that PIRATA achieve the "moderate quality" pyranometer measurements defined by WMO (2008, rev. 2012), one may ask if these data sets are compliant with "moderate quality" if one may remove the bias. Defined as the 95% probability (P95), the relative uncertainty for "moderate quality" should not exceed 20%. The total uncertainty takes into account the uncertainty of PIRATA and the uncertainty of the estimates. It can be expressed in a first approximation as the quadratic sum of both uncertainties. As a consequence, the total relative uncertainty should not exceed 28% (P95), or 14% (P66) if the estimates were of "moderate" quality. The standard deviations (P66) for each data set reported in Table 3 are below 14%. It can be concluded that to a first approximation, the three satellite-derived data sets can be considered of moderate quality if bias can be removed.

One may note several similarities in performances between HC3v5 and SARAH-2. It is speculated that this is partly due to the fact that they exploit the same method, Heliosat-2, though the implementation differs.

The three satellite-derived data sets are appropriate to study the dynamics of the downward solar irradiance at the surface of the tropical Atlantic Ocean. Their performances are fairly similar. The CRS exhibit the lowest biases. When the study of the

irradiance field is at stake, one should prefer HC3v5 as the bias is fairly similar from one location to the other which means that the actual spatial gradients are well reproduced.

Other data sets are available that cover the tropical Atlantic Ocean and must be assessed against the PIRATA measurements to gain knowledge on their limitations and confidence in their use. Examples are the satellite-derived OSI-SAF (www.osi-saf.org) or the Japanese 55-year re-analysis (JRA 55, Kang et al., 2015; Kobayashi et al., 2015).

The findings reported here are similar to those already published. This demonstrates a posteriori that the PIRATA measurements may be used for the validation of models and data sets. However, some uncertainties remain: It is striking that all satellite-based data records show their lowest correlation at the same buoy location, i.e. 19s34w. While the different levels and variability of surface irradiance in this location might impact the quality of the satellite-based data sets, a reduced data quality of the buoy data (despite the quality control applied) might also have an impact on the presented evaluation. Studies like these when multiple data records are considered can help to identify problem in surface reference measurements (Urraca et al., 2017). The PIRATA network is a unique and valuable means to study and monitor the surface irradiance in the tropical Atlantic Ocean and deserves support for operations to further enrich the data records.

Data availability

PIRATA measurements performed every 2 min were downloaded from the web site (www.pmel.noaa.gov/tao/drupal/disdel/) of the National Oceanic and Atmospheric Administration (NOAA) of the U.S.A. The authors acknowledge the help of the GTMBA Project Office of NOAA/PMEL in getting the data and the PIRATA team for servicing the network and freely providing the data.

Time-series of HelioClim-3v5 data were downloaded from the SoDa Service web site (www.soda-pro.com) managed by the company Transvalor. Data are available to anyone for free for years 2004-2006 as a GEOSS Data-CORE (GEOSS Data Collection of Open Resources for Everyone) and for a charge for the most recent years with the amount depending on requests and requester. The time-series used in this article are available for free in CSV format by request to Mireille Lefèvre.

Time-series of SARAH-2 data were extracted from the gridded data sets available at https://doi.org/10.5676/EUM_SAF_CM/SARAH/V002.

Time-series of CAMS Radiation Service data were downloaded from the SoDa Service web site (www.soda-pro.com).

Time-series of cloud classification were downloaded from the SoDa Service web site (www.soda-pro.com).

MERRA-2 times-series were extracted from the gridded data sets available at https://goldsmr4.gesdisc.eosdis.nasa.gov/data/MERRA2/.

ERA-5 times-series were extracted from the gridded data sets available at http://apps.ecmwf.int/data-catalogues/era5/?class=ea&stream=enda&expver=1.

Author contribution

All authors contributed equally to this work.

Competing interests

The authors declare no competing interests.

Disclaimer

N/A

Acknowledgements

The research leading to these results has partly received funding from the Copernicus Atmosphere Monitoring Service, a program being operated by the European Centre for Medium-Range Weather Forecasts (ECMWF) on behalf of the European Union. The authors thank the French company Transvalor, which takes care of the SoDa Service for the common good, thus providing an efficient access to the HelioClim databases. The authors thank especially Gregory Foltz for his helpful advices on the PIRATA measurements.

References

Bengulescu, M., Blanc, P., Boilley, A., and Wald, L.: Do modelled or satellite-based estimates of surface solar irradiance accurately describe its temporal variability?, Adv Sci Res, 14, 35-48, doi:10.5194/asr-14-35-2017, 2017.

Blanc, P., and Wald L.: The SG2 algorithm for a fast and accurate computation of the position of the Sun, Sol Energy, 86, 3072-3083, doi: 10.1016/j.solener.2012.07.018, 2012.

Boilley, A., and Wald, L.: Comparison between meteorological re-analyses from ERA-Interim and MERRA and measurements of daily solar irradiation at surface, Renew Energ, 75, 135-143, doi: 10.1016/j.renene.2014.09.042, 2015.

Bourlès, B., Lumpkin, R., McPhaden, M. J., Hernandez, F., Nobre, P., Campos, E., Yu, L., Planton, S., Busalacchi, A., Moura, A. D., Servain, J., and Trotte, J.: The Pirata Program: History, accomplishments, and future directions, B Am Meteorol Soc, 89, 1111–1125, doi:10.1175/2008BAMS2462.1, 2008.

Budyko, M. I.: The effect of solar radiation variations on the climate of the Earth, Tellus, 21, 611-619, doi:10.1111/j.2153-3490.1969.tb00466.x, 1969.

Cros, S., Mayer, D., and Wald, L.: The Availability of Irradiation Data. Report IEA-PVPS T2-04: 2004, International Energy Agency, Vienna, Austria, 29 p., 2004.

Doddy, E., Sweeney, C., McDermott, F.: An investigation of systematic errors in solar radiation from reanalysis datasets. EMS Annual Meeting 2017, Dublin, Ireland, 4-8 September 2017. Abstract EMS2017-675.

Eissa, Y., Munawwar, S., Oumbe, A., Blanc, P., Ghedira, H., Wald, L., Bru, H., and Goffe, D.: Validating surface downwelling solar irradiances estimated by the McClear model under cloud-free skies in the United Arab Emirates, Sol Energy, 114, 17-31, doi:10.1016/j.solener.2015.01.017, 2015.

Foltz, G. R., Evan, A. T., Freitag, H. P., Brown, S., and McPhaden, M. J.: Dust accumulation biases in PIRATA shortwave radiation records, J Atmos Ocean Technol, 30, 1414–1432, doi: 10.1175/JTECH-D-12-00169.1, 2013.

Gelaro, R., McCarty, W., Suárez, M.J., Todling, R., Molod, A., Takacs, L., Randles, C.A., Darmenov, A., Bosilovich, M.G., Reichle, R., Wargan, K., Coy, L., Cullather, R., Draper, C., Akella, S., Buchard, V., Conaty, A., da Silva, A.M., Gu, W., Kim, G., Koster, R., Lucchesi, R., Merkova, D., Nielsen, J.E., Partyka, G., Pawson, S., Putman, W., Rienecker, M., Schubert, S.D., Sienkiewicz, M., and Zhao, B.: The modern-era retrospective analysis for research and applications, Version 2 (MERRA-2), J Climate, 30, 5419–5454, doi: 10.1175/JCLI-D-16-0758.1, 2017.

Gschwind, B., Ménard, L., Albuisson, M., and Wald, L.: Converting a successful research project into a sustainable service: the case of the SoDa Web service, Environ Modell Softw, 21, 1555-1561, doi:10.1016/j.envsoft.2006.05.002, 2006.

Hersbach, H., and Dee, D.: ERA5 reanalysis is in production, ECMWF Newsletter No. 147, p. 7, 2016.

ISO Guide to the Expression of Uncertainty in Measurement: first edition, International Organization for Standardization, Geneva, Switzerland, 1995.

Jones, P., Harpham, C., Troccoli, A., Gschwind, B., Ranchin, T., Wald, L., Goodess, C., and Dorling, S.: Using ERA-Interim reanalysis for creating datasets of energy-relevant climate variables, Earth System Science Data, 9, 471-495, 10.5194/essd-9-471-2017, 2017.

Kang, S., and Ahn, JB.: Global energy and water balances in the latest reanalyses, Asia-Pacific J Atmos Sci, 51, 293-302, doi: 10.1007/s13143-015-0079-0, 2015.

Katsaros, K. B., and DeVault, J. E.: On irradiance measurement errors at sea due to tilt of pyranometers, J Atmos Ocean Tech, 3, 740-745, doi: 10.1175/1520-0426(1986)003<0740:OIMEAS>2.0.CO;2, 1986.

Kennedy, A. D., Dong, X., Xi, B., Xie, S., Zhang, Y., and Chen, J.: A comparison of MERRA and NARR reanalyses with the DOE ARM SGP data, J Climate, 24, 4541–4557, doi: 10.1175/2011JCLI3978.1, 2011.

Kobayashi, S., Ota, Y., Harada, Y., Ebita, A., Moriya, M., Onoda, H., Onogi, K., Kamahori, H., Kobayashi, C., Endo, H., Miyaoka, K., and Takahashi, K.: The JRA-55 Reanalysis: General specifications and basic characteristics, J Meteor Soc Japan, 93, 5-48, doi:10.2151/jmsj.2015-001, 2015.

Korany, M., Boraiy, M., Eissa, Y., Aoun, Y., Abdel Wahab, M. M., Alfaro, S. C., Blanc, P., El-Metwally, M., Ghedira, H., Hungershoefer, K., and Wald, L.: A database of multi-year (2004-2010) quality-assured surface solar hourly irradiation measurements for the Egyptian territory, Earth Syst Sci Data, 8, 105–113, doi:10.5194/essd-8-105-2016, 2016.

Koster, R. (editor): Technical Report Series on Global Modeling and Data Assimilation, Volume 43, National Aeronautics and Space Administration (NASA), 139 p., 2015.

Lean, J., and Rind, D.: Climate forcing by changing solar radiation, J Climate, 11, 3069–3094, doi: 10.1175/1520-0442(1998)011<3069:CFBCSR>2.0.CO;2, 1998.

Lefèvre, M., and Wald, L.: Validation of the McClear clear-sky model in desert conditions with three stations in Israel, Adv Sci Res, 13, 21-26, doi:10.5194/asr-13-21-2016, 2016.

Lefèvre, M., Diabaté, L., and Wald, L.: Using reduced data sets ISCCP-B2 from the Meteosat satellites to assess surface solar irradiance, Sol Energy, 81, 240-253, doi:10.1016/j.solener.2006.03.008, 2007.

Lefèvre, M., Oumbe, A., Blanc, P., Espinar, B., Gschwind, B., Qu, Z., Wald, L., Schroedter-Homscheidt, M., Hoyer-Klick, C., Arola, A., Benedetti, A., Kaiser, J. W., and Morcrette, J.-J.: McClear: a new model estimating downwelling solar radiation at ground level in clear-sky condition, Atmos Meas Tech, 6, 2403-2418, doi: 10.5194/amt-6-2403-2013, 2013.

Lefèvre, M., Blanc, P., Espinar, B., Gschwind, B., Ménard, L., Ranchin, T., Wald, L., Saboret, L., Thomas, C., and Wey, E.: The HelioClim-1 database of daily solar radiation at Earth surface: an example of the benefits of GEOSS Data-CORE, IEEE JSTARS, 7, 1745-1753, doi:10.1109/JSTARS.2013.2283791, 2014.

Liu, C., Allan, R. P., Mayer, M., Hyder, P., Loeb, N. G., Roberts, C. D., Valdivieso, M., Edwards, J. M., and Vidale, P.-L.: Evaluation of satellite and reanalysis based global net surface energy flux and uncertainty estimates, J Geophys Res Atmos, 122, doi:10.1002/2017JD026616, 2017.

Long, C. N., Bucholtz, A., Jonsson, H., Schmid, B., Vogelmann, A., and Wood, J.: A method of correcting for tilt from horizontal in downwelling shortwave irradiance measurements on moving platforms, The Open Atmospheric Science Journal, 4, 78-87, doi: 10.2174/1874282301004010078, 2010.

MacWhorter, M. A., and Weller, R. A.: Error in measurements of incoming shortwave radiation made from ships and buoys, J Atmos Ocean Tech, 8, 108-117, doi: 10.1175/1520-0426(1991)008<0108:EIMOIS>2.0.CO;2, 1991.

Manabe, S.: Climate and the ocean circulation, Mon Wea Rev, 97, 739-774, doi:10.1175/1520-0493(1969)097<0739:CATOC>2.3.CO;2, 1969.

Marchand, M., Al-Azri, N., Ombe-Ndeffotsing, A., Wey, E., and Wald, L.: Evaluating meso-scale change in performance of several databases of hourly surface irradiation in South-eastern Arabic Peninsula, Adv Sci Res, 14, 7-15, doi:10.5194/asr-14-7-2017, 2017.

Müller, R., Pfeifroth, U., Traeger-Chatterjee, C., Trentmann, J. and Cremer, R.: Digging the METEOSAT treasure-3 decades of solar surface radiation, Remote Sens-Basel, 7, 8067-8101, doi:10.3390/rs70608067, 2015.

Muneer, T., and Fairooz, F.: Quality control of solar radiation and sunshine measurements - lessons learnt from processing worldwide databases, Build Serv Eng Res T, 23, 151-166, doi: 10.1191/0143624402bt038oa, 2002.

Pfeifroth, U., Kothe, S., Müller, R., Trentmann, J., Hollmann, R., Fuchs, P., and Werscheck M.: Surface Radiation Data Set - Heliosat (SARAH) - Edition 2. Satellite Application Facility on Climate Monitoring. doi: 10.5676/EUM_SAF_CM/SARAH/V002, 2017a.

Pfeifroth, U., Sanchez-Lorenzo, A., Manara, V., Trentmann, J., and Hollmann, R.: Trends and variability of surface solar radiation in Europe based on surface- and satellite-based data records, J Geophys Res, under review, 2017b.

Qu, Z., Gschwind, B., Lefèvre, M., and Wald, L.: Improving HelioClim-3 estimates of surface solar irradiance using the McClear clear-sky model and recent advances in atmosphere composition, Atmos Meas Tech, 7, 3927–3933, doi:10.5194/amt-73927-2014, 2014.

Qu, Z., Oumbe, A., Blanc, P., Espinar, B., Gesell, G., Gschwind, B., Klüser, L., Lefèvre, M., Saboret, L., Schroedter-Homscheidt, M., and Wald L.: Fast radiative transfer parameterisation for assessing the surface solar irradiance: The Heliosat-4 method, Meteorologische Zeitschrift, 26, 33-57, doi:10.1127/metz/2016/0781, 2017.

Reynolds, R. M.: Correcting global shortwave irradiance measurements for platform tilt, Internal Report, RMR Company, available at www.rmrco.com/docs/m0703_psp_lowlevel_correction.pdf, last accessed: 2017-07-28.

Rienecker, M. M., Suarez, M. J., Gelaro, R., Todling, R., Bacmeister, J., Liu, E., Bosilovich, M. G., Schubert, S. D., Takacs, L., Kim, G.-K., Bloom, S., Chen, J., Collins, D., Conaty, A., da Silva, A., Gu, W., Joiner, J., Koster, R. D., Lucchesi, R., Molod, A., Owens, T., Pawson, S., Pegion, P., Redder, C. R., Reichle, R., Robertson, F. R., Ruddick, A. G., Sienkiewicz, M., and Woollen, J.: MERRA: NASA's modern-era retrospective analysis for research and applications, J Climate, 24, 3624-3648, doi:10.1175/JCLI-D-11-00015.1, 2011.

Rigollier, C., Lefèvre, M., and Wald, L.: The method Heliosat-2 for deriving shortwave solar radiation from satellite images, Sol Energy, 77, 159-169, doi 10.1016/j.solener.2004.04.017, 2004.

Siegel, D. A., Ohlmann, J. C., Washburn, L., Bidigare, R. R., Nosse, C. T., Fields, E., and Zhou, Y.: Solar radiation, phytoplankton pigments and the radiant heating of the equatorial Pacific warm pool, J Geophys Res, 100(C3), 4885–4891, doi:10.1029/94JC03128, 1995.

Thomas, C., Wey, E., Blanc, P., and Wald, L.: Validation of three satellite-derived databases of surface solar radiation using measurements performed at 42 stations in Brazil, Adv Sci Res, 13, 81-86, doi:10.5194/asr-13-81-2016, 2016a.

Thomas, C., Wey, E., Blanc, P., Wald, L., and Lefèvre, M.: Validation of HelioClim-3 version 4, HelioClim-3 version 5 and MACC-RAD using 14 BSRN stations, Energy Procedia, 91, 1059-1069, doi: 10.1016/j.egypro.2016.06.275, 2016b.

Urraca, R., Gracia-Amillo, A. M., Huld, T., Martinez-de-Pison, F. J., Trentmann, J., Lindfors, A. V., Riihelä, A., and Sanz-Garcia, A.: Quality control of global solar radiation data with satellite-based products, Solar Energy, 158, 49-62, doi: 10.1016/j.solener.2017.09.032, 2017.

Wald L.: Solar radiation energy (fundamentals). In Solar Energy Conversion and Photoenergy Systems, edited by Julian Blanco and Sixto Malato, in Encyclopedia of Life Support Systems (EOLSS), Developed under the Auspices of the UNESCO, Eolss Publishers, Oxford ,UK, [http://www.eolss.net], 2007.

Wild, M.: Short-wave and long-wave surface radiation budgets in GCMs: a review based on the IPCC-AR4/CMIP3 models, Tellus, 60A, 932–945, doi: 10.1111/j.1600-0870.2008.00342.x, 2008.

WMO: Guide to meteorological instruments and methods of observation, WMO-No 8, 2008 edition updated in 2010, World Meteorological Organization, Geneva, Switzerland, 2012.

Yi, Y., Kimball, J.S., Jones, L.A., Reichle, R.H., and McDonald, K.C.: Evaluation of MERRA land surface estimates in preparation for the soil moisture active passive mission, J Climate, 24, 3797-3816, doi: 10.1175/2011JCLI4034.1, 2011.

Zib, B. J., Dong, X., Xi, B., and Kennedy, A.: Evaluation and intercomparison of cloud fraction and radiative fluxes in recent reanalyses over the Arctic using BSRN surface observations, J Climate, 25, 2291–2305, doi: 10.1175/JCLI-D-11-00147.1, 2012.

Zhao, L., Lee, X., and Liu, S.: Correcting surface solar radiation of two data assimilation systems against FLUXNET observations in North America, J Geophys Res Atmos, 118, 9552–9564, doi:10.1002/jgrd.50697, 2013.

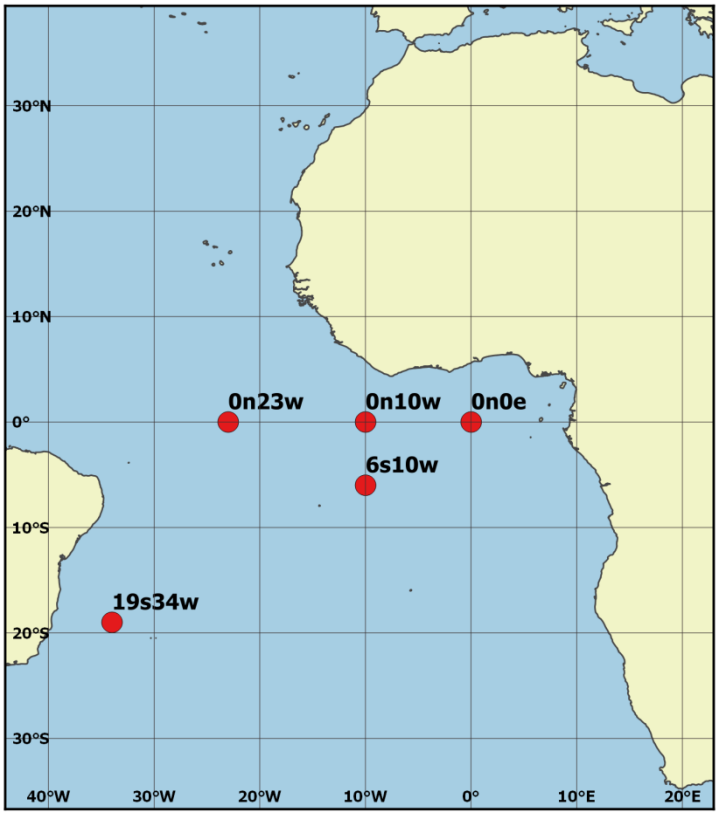

Figure 1: Map showing the location of the five PIRATA buoys used in this study.

Ocean Sci. Discuss., https://doi.org/10.5194/os-2017-95
Manuscript under review for journal Ocean Sci.
Discussion started: 18 December 2017

(a)

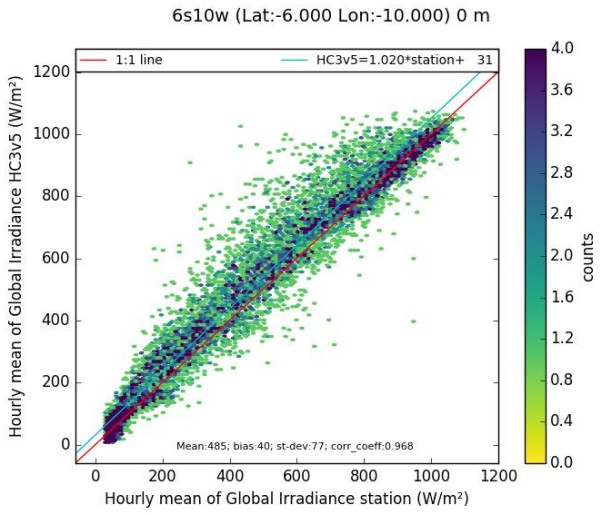

(b)

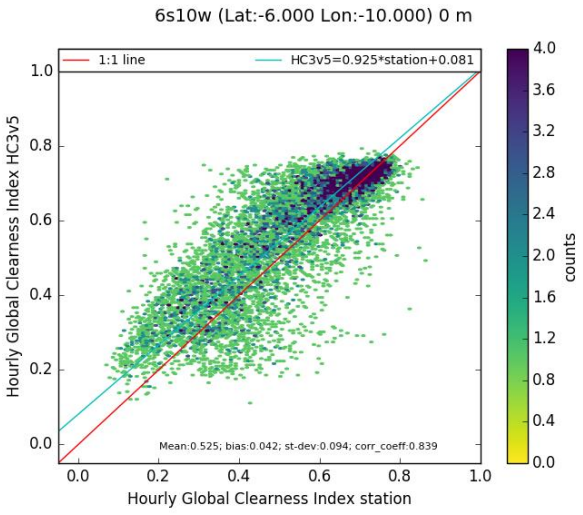

(c)

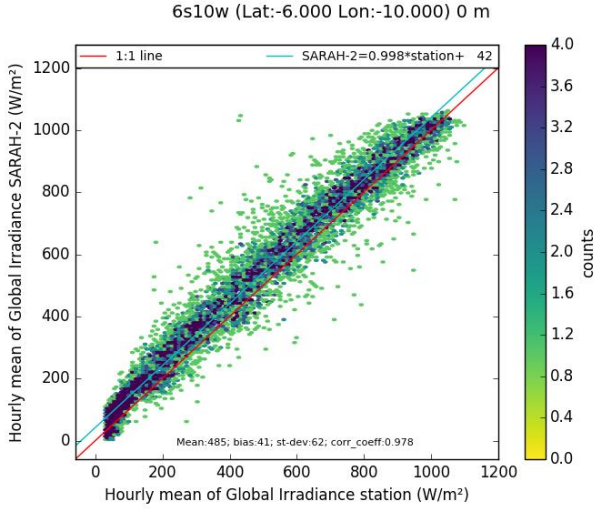

(d)

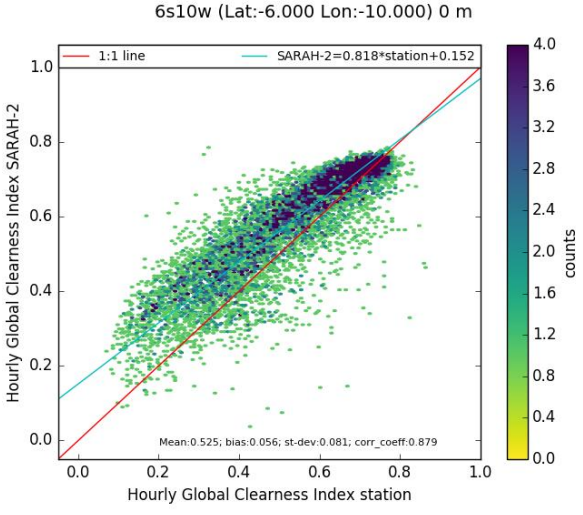

Ocean Sci. Discuss., https://doi.org/10.5194/os-2017-95
Manuscript under review for journal Ocean Sci.
Discussion started: 18 December 2017

(e)

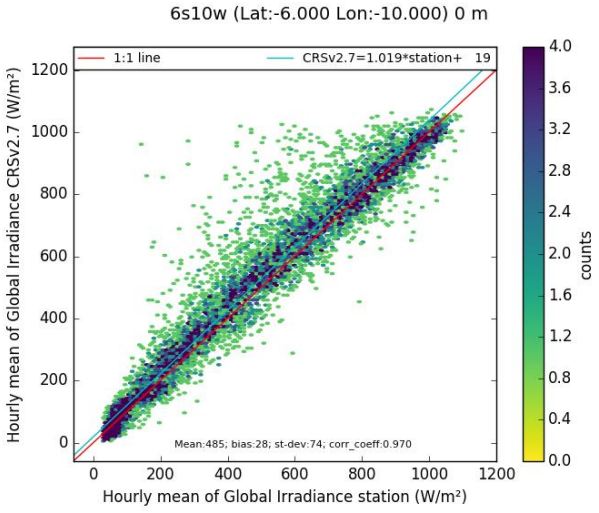

(f)

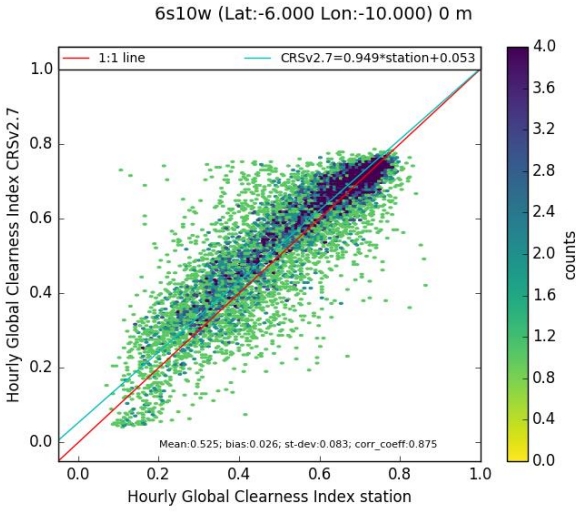

(g)

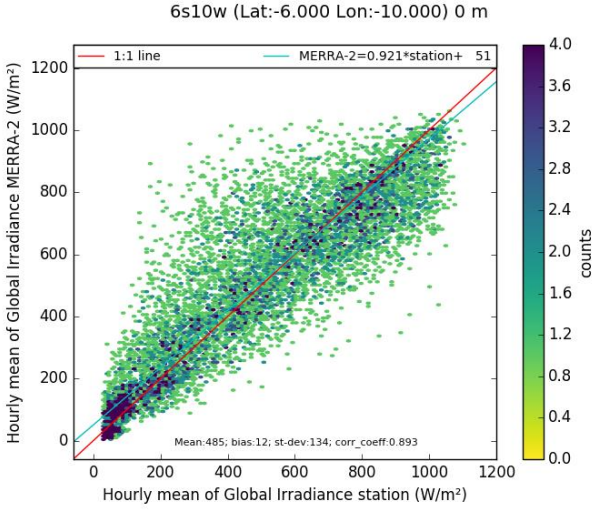

(h)

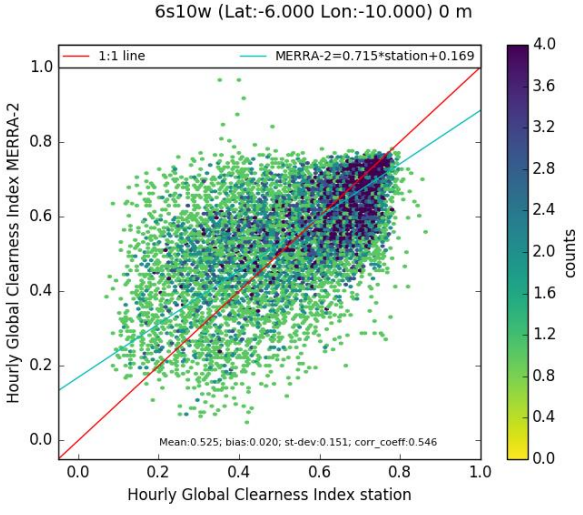

Ocean Sci. Discuss., https://doi.org/10.5194/os-2017-95
Manuscript under review for journal Ocean Sci.
Discussion started: 18 December 2017

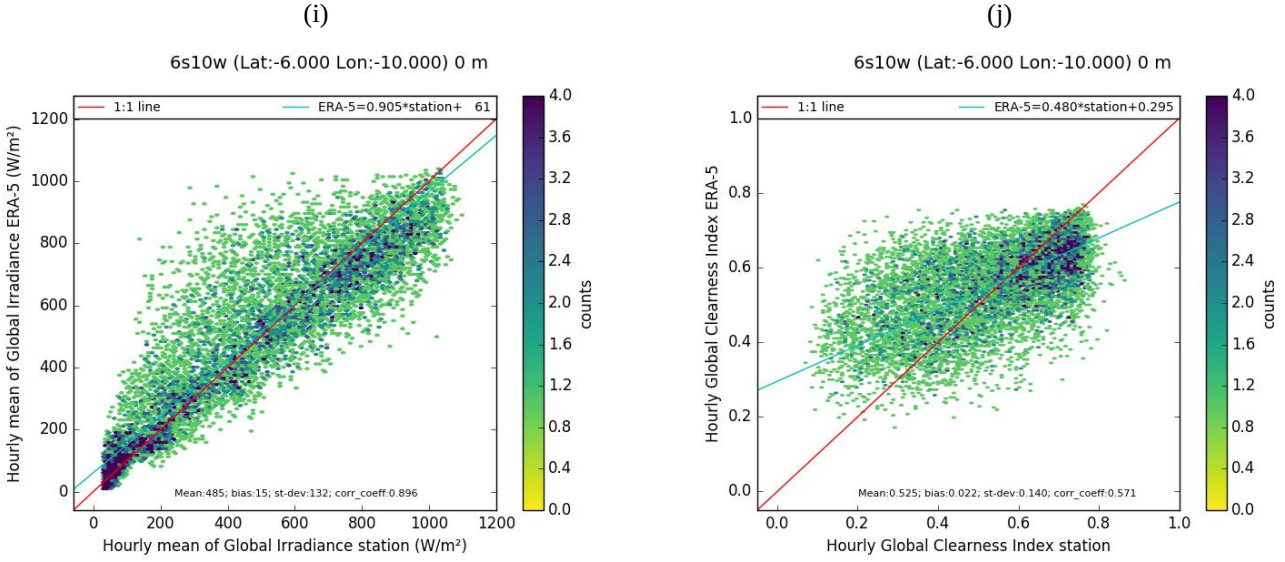

Figure 2: 2D histogram of PIRATA measurements (horizontal axis) and data sets (vertical axis) for the station 6s10w for E (left) and KT (right). HC3v5: (a), (b); SARAH 2: (c), (d); CRS: (e), (f); MERRA-2: (g), (h); ERA-5: (i), (j). Ideally, the dots should lie along the red line (1:1 line). The blue line is the affine function fitted over the points and should overlay the red line.

5

Ocean Sci. Discuss., https://doi.org/10.5194/os-2017-95
Manuscript under review for journal Ocean Sci.
Discussion started: 18 December 2017

(a)

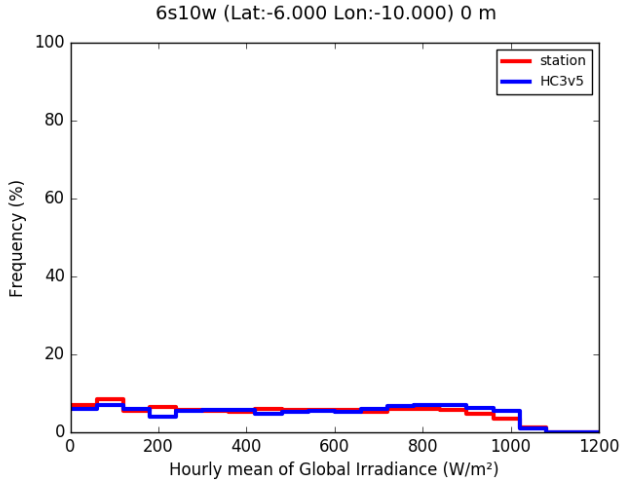

(b)

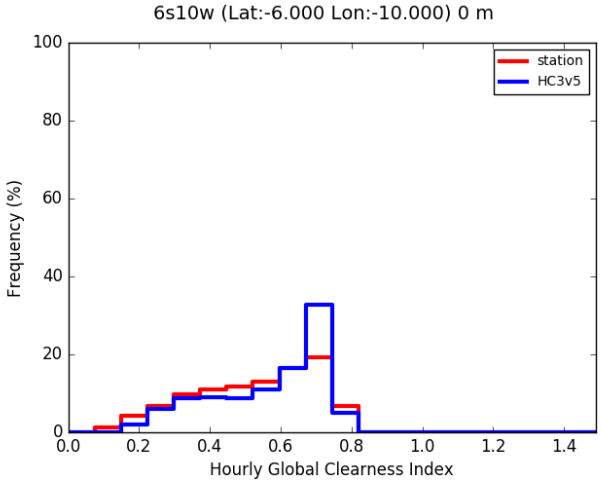

(c)

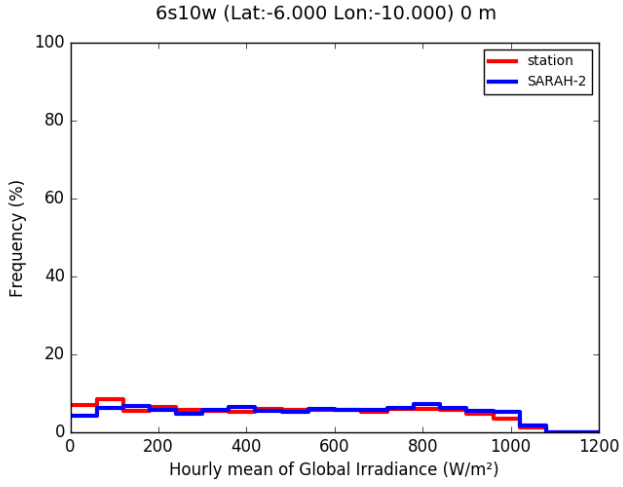

(d)

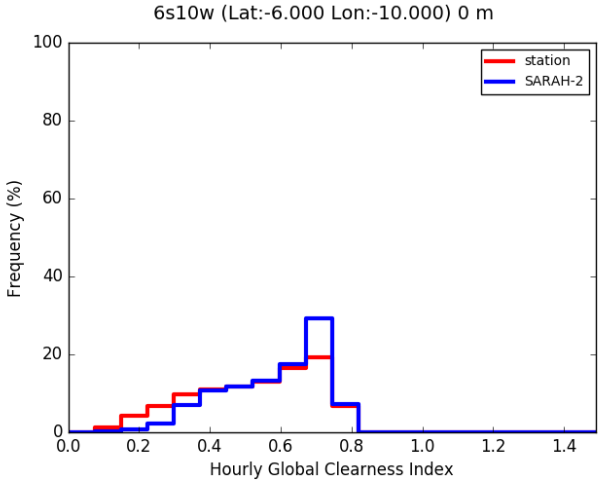

Ocean Sci. Discuss., https://doi.org/10.5194/os-2017-95
Manuscript under review for journal Ocean Sci.
Discussion started: 18 December 2017

(e)

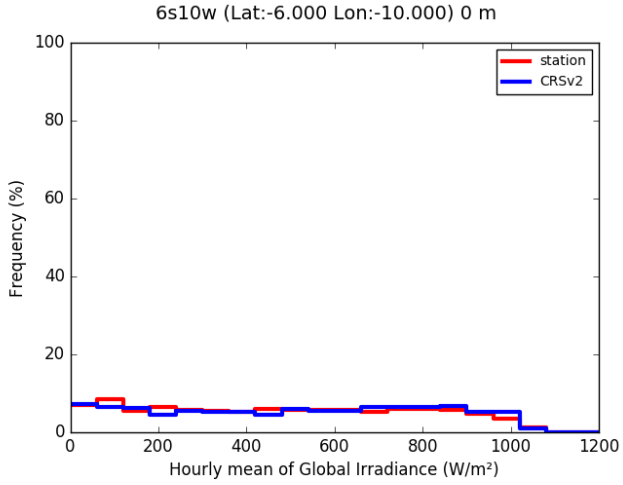

(f)

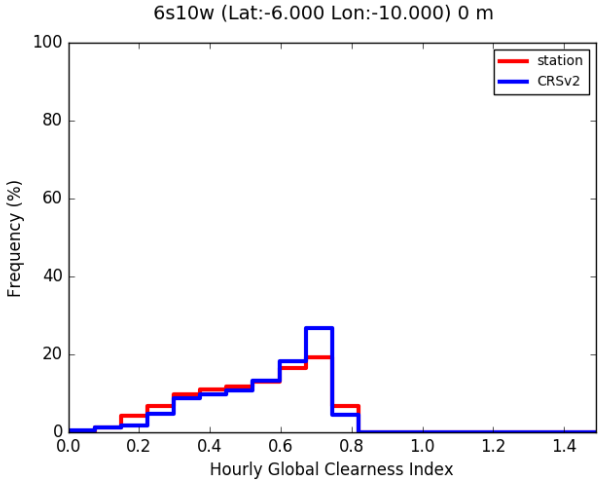

(g)

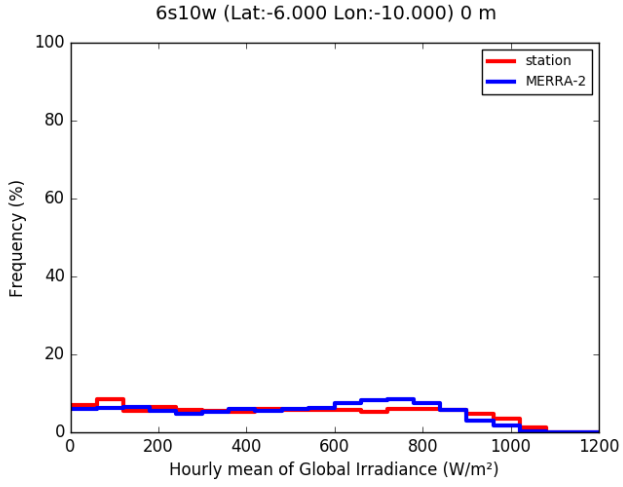

(h)

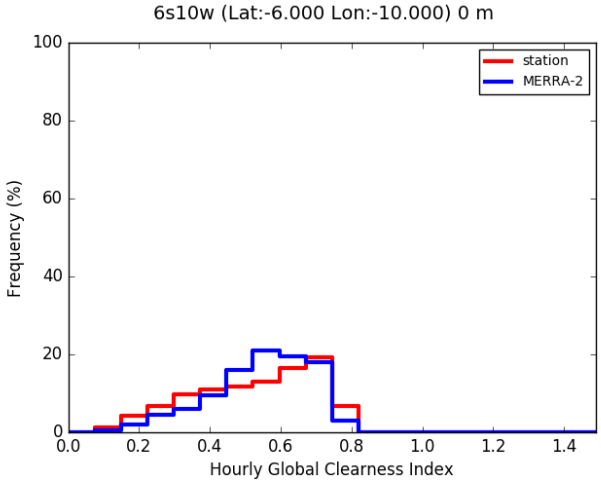

Ocean Sci. Discuss., https://doi.org/10.5194/os-2017-95
Manuscript under review for journal Ocean Sci.
Discussion started: 18 December 2017

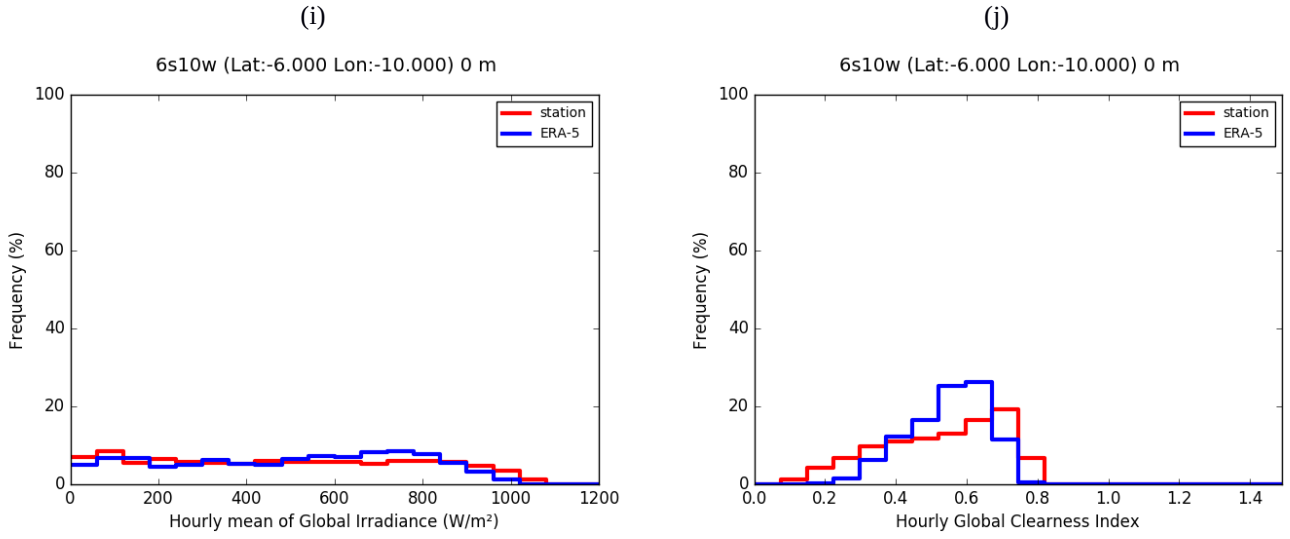

Figure 3: Frequency distributions of PIRATA measurements (red) and data sets (blue) for the station 6s10w for E (left) and KT (right). HC3v5: (a), (b); SARAH 2: (c), (d); CRS: (e), (f); MERRA-2: (g), (h); ERA-5: (i), (j). If the blue line is above, respectively below, the red one for a given sub-range of values, it means that the data set produces these values too frequently, respectively too rarely with respect to the PIRATA measurements.

5

Ocean Sci. Discuss., https://doi.org/10.5194/os-2017-95
Manuscript under review for journal Ocean Sci.
Discussion started: 18 December 2017

(a)

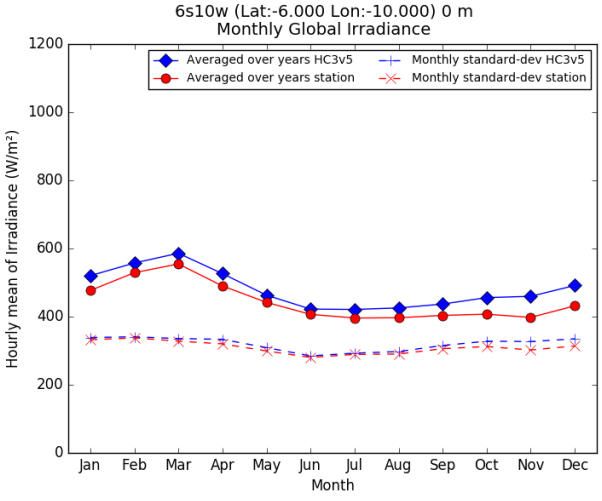

(b)

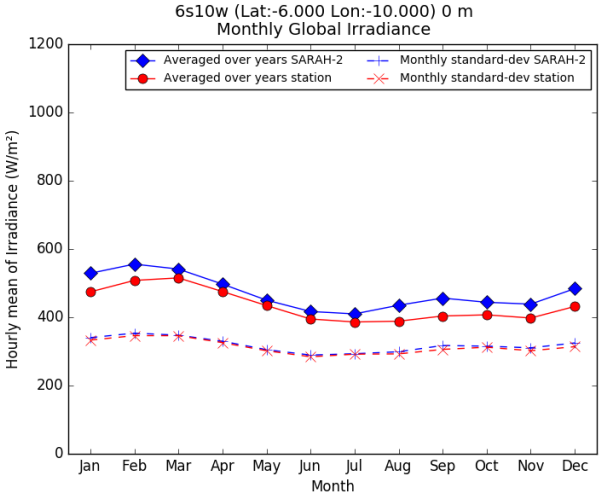

Ocean Sci. Discuss., https://doi.org/10.5194/os-2017-95
Manuscript under review for journal Ocean Sci.
Discussion started: 18 December 2017

(c)

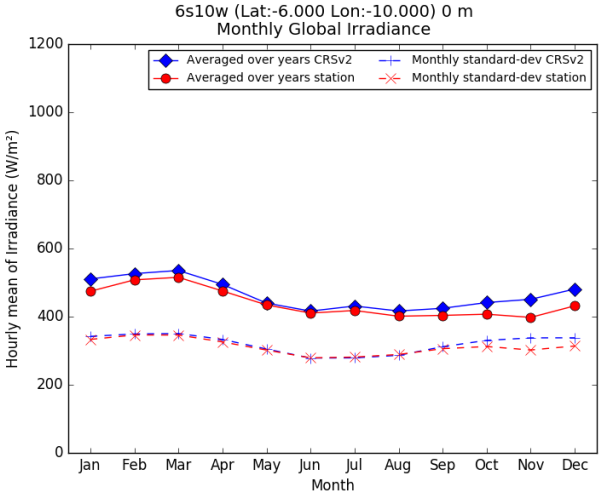

(d)

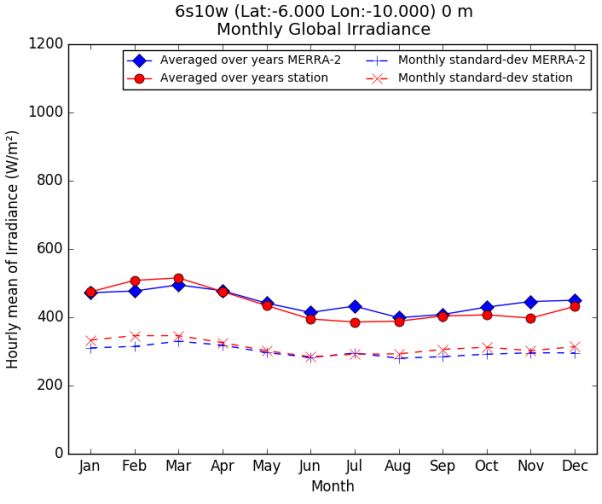

Ocean Sci. Discuss., https://doi.org/10.5194/os-2017-95
Manuscript under review for journal Ocean Sci.
Discussion started: 18 December 2017

(e)

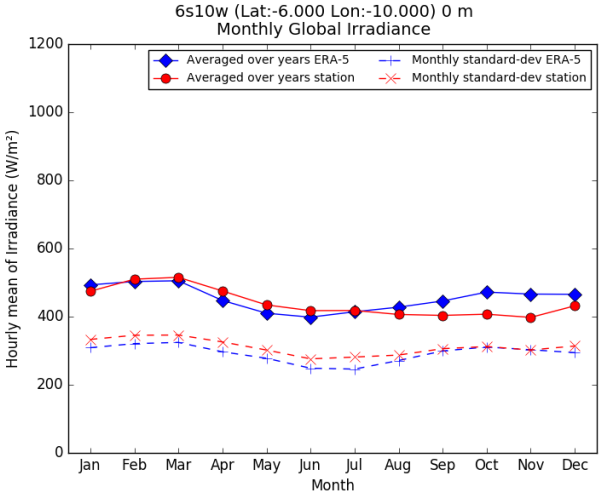

Figure 4: Monthly means (dots) and standard deviations (crosses) of hourly DSIS, in W m 2, from PIRATA measurements (red) and data sets (blue) for the station 6s10w. HC3v5: (a); SARAH 2: (b); CRS: (c); MERRA-2: (d); ERA-5: (e). A difference between red dot (measurements) and blue diamond (data set) for a given month denotes a systematic error for this month: underestimation if the blue diamond is below the red dot, overestimation otherwise. For a given month, a blue cross above the red one means that the data set produces too much variability for this month; in the opposite case, the data set does not contain enough variability.

Ocean Sci. Discuss., https://doi.org/10.5194/os-2017-95
Manuscript under review for journal Ocean Sci.
Discussion started: 18 December 2017

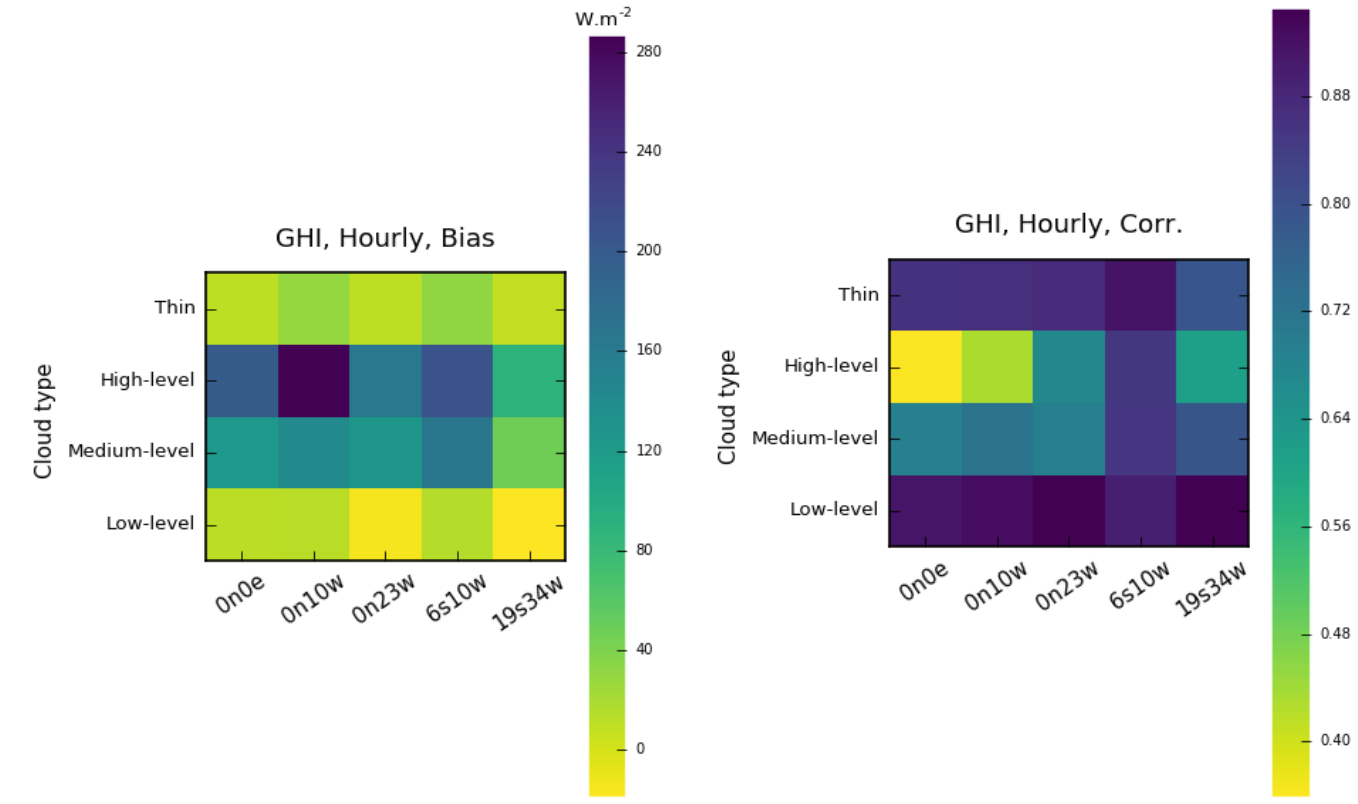

Ocean Sci. Discuss., https://doi.org/10.5194/os-2017-95
Manuscript under review for journal Ocean Sci.
Discussion started: 18 December 2017

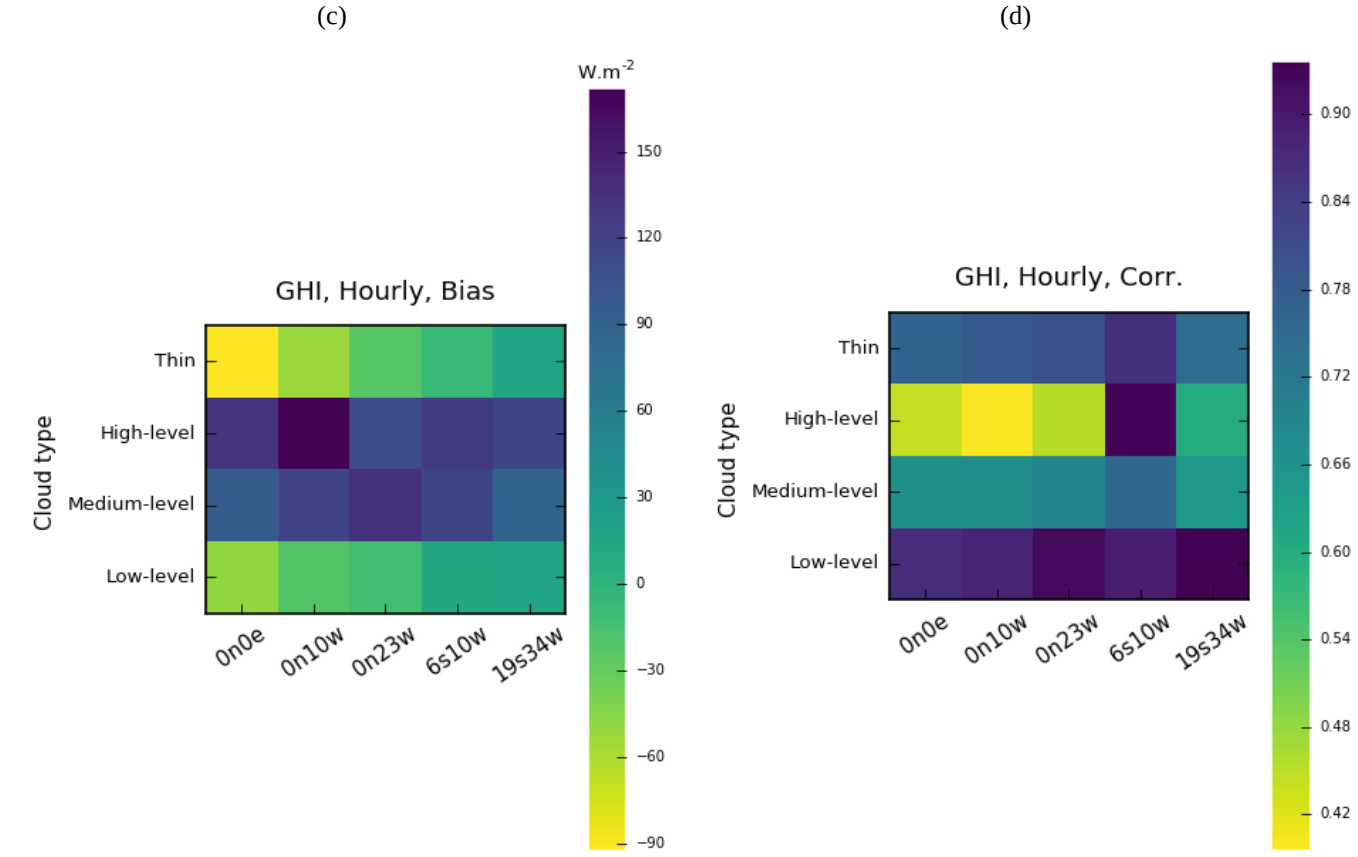

Figure 5: Bias (left, in W m 2) and correlation coefficient (right) as a function of the cloud type for each PIRATA station. ERA-5: (a), (b); MERRA-2: (c), (d). A plot should be uniformly colored in case of no dependency.